MATERIALS AND STRUCTURES FOR HYPERSONIC VEHICLES

D. R. Tenney, W. B. Lisagor, and S. C. Dixon
NASA Langley Research Center
Hampton, Virginia

Abstract

The development of low-density materials with higher strength and stiffness, and more efficient engine and airframe structures is considered enabling technology for reusable hypersonic vehicles. Advanced structural concepts are required for minimum weight hot structures that will be fully reusable. Key design drivers are maximum heating rate, duration of heating, total heat load, flight envelope and type of propulsion system, mission life requirements, and containment of liquid hydrogen. For hot-structures applications in the range from 600-1800°F, advanced alloys of titanium, titanium and nickel aluminides, and metal-matrix composites are leading candidates because of their high specific properties. For temperatures in excess of 2000°F carbon-carbon and ceramic-matrix composites are the most structurally efficient materials. This paper addresses the technology issues for light weight hot structures, gives brief assessments of the state of the art, presents selected highlights of current research, and identifies areas requiring additional development.

I. Introduction

Reusable hypersonic flight vehicles have been of interest to NASA and the Air Force for more than three decades. The U.S. had extensive programs in the 1950's and early 1960's paimed at various missions requiring flight of reusable vehicles at hypersonic speeds [1-8]. Although most of the missions were of a military nature, civil programs such as supersonic and hypersonic transports were also studied. Due to accelerating cost and formidable technical challenges most programs were terminated, and except for the NASA Space Shuttle Program, R&T for hypersonic vehicles has been a low priority effort. However, a low level of research on key technologies such as materials, structures, aerothermodynamics, propulsion, structural heat transfer, and hypersonic air-breathing propulsion was continued by NASA mainly at the Langley Research Center. The key results of that work are summarized in References 9-19.

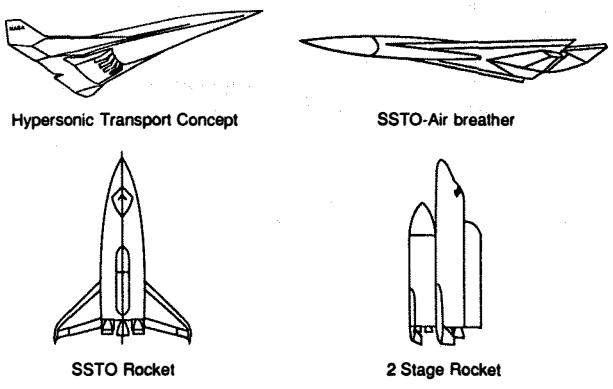

Figure 1. Future fully reusable hypersonic vehicles.

The four most commonly proposed fully reusable configurations for hypersonic vehicles are shown in Figure 1. Rocket powered vehicles, both single-stage-to-orbit (SSTO) and two-stage systems,will be launched vertically whereas the air breathing vehicles will take off horizontally. All will land horizontally. Liquid hydrogen appears to be the choice of fuel, thus all vehicles will have large cryogenic tanks that will occupy the major portion of the vehicle's volume. The ascent, reentry, and cruise flight envelopes of these vehicles compared to current aircraft are shown in Figure 2. For rocket-powered space transportation systems, such as the Space Shuttle, reentry conditions are more severe than ascent conditions and require that the vehicle have the capability to withstand temperatures up to 3000°F. Concepts to withstand high temperatures include: 1) use a thermal protection system, such as used on the Shuttle, to protect a conventional aluminum airframe (restricted to 350°F max.); 2) actively cool the structure; or 3) design with a hot airframe using high-temperature materials.

For air breathing space transportation vehicles, the ascent trajectory is the most severe and dominates design requirements for the vehicle. The air breathing ascent trajectory is primarily set to establish propulsion efficiency, but is constrained by the maximum temperature that the vehicle can withstand. Most studies indicate that the nosecap, leading edges, and portions of the engine and airframe of air breathing vehicles will have to be actively cooled during ascent. The high heating during ascent also imposes formidable sealing problems for doors, windows, control surfaces, etc. However, the theoretical efficiency of the air breathing engine is much greater than for rocket engines and thus warrants exploiting in future vehicles. Structures and materials technology applicable to such air breathing vehicles is being developed in the National Aero-Space Plane (NASP) program. A typical NASP configuration is shown in Figure 1. It is a blended wing-body configuration with scramjet engines which

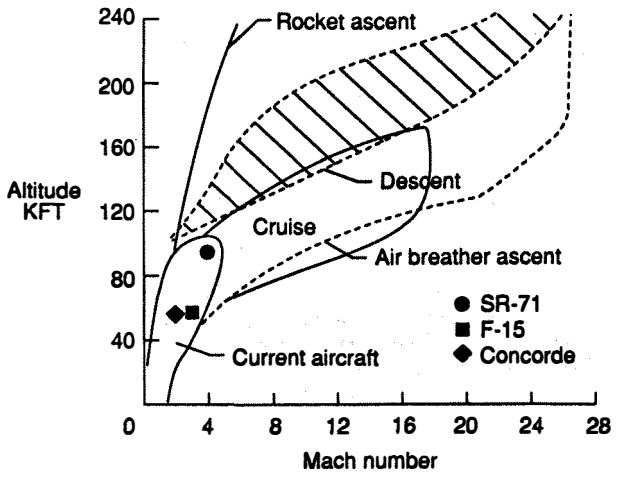

Figure 2. Ascent, reentry, and cruise envelope.

use the fuselage forebody as the engine "inlet surface." The hydrogen fuel would be used to cool portions of the engine and the airframe which experience the most severe aerodynamic heating. Such vehicles[20] will require structural weight fractions that are much lower than those of todays aerospace vehicles.

Large areas of the structure will be subjected to equilibrium skin temperatures of 2500°F or higher, unless actively cooled. Conventional high-temperature materials such as superalloys, coated refractory metals, and monolithic ceramics have significant drawbacks for hypersonic airframe structures because of such factors as limited strength and stiffness, relatively high density, brittle nature, and susceptibility to thermal shock. Emerging high-temperature, low-density materials such as coated carbon-carbon composites, aluminide intermetallic composites, and ceramic-matrix composites hold promise to provide the properties required to meet mission goals of multiple high Mach number flights. However, extensive efforts in materials development, process development, scaleup, fabrication technologies, property characterization, and proof-of-concept studies must be undertaken to provide hypersonic vehicle designers with confidence in such materials.

The NASP program has recently focused the attention of the American aerospace industry on the technology challenges of hypersonic airframes and scramjet engines. Structures and materials technology needs for hypersonic cruise vehicles have emerged from systems studies. This paper presents highlights of the materials and structures research programs conducted at the NASA Langley Research Center in support of NASA's hypersonic vehicles technology program.

II. Structural Concepts

The wide range of hypersonic vehicles and missions introduces a number of design requirements which lead to a variety of structural concepts and materials systems. The range of structural concepts and materials is reduced if the missions of interest are restricted to those requiring reusable vehicles, but even with this restriction, the number of design drivers is large:

1) Maximum heating rate, duration of heating, total heat load
2) Flight envelope and type of propulsion system
3) Mission life requirements
4) Containment of cryogens, especially liquid hydrogen (LH_2) and liquid oxygen (LOX)
5) Effect of structural mass on mission goals

Design Driver 2 relates to air-breathing propulsion and earth-to-orbit vehicles, such as the National Aero-Space Plane, which need to fly a high dynamic pressure and high Mach number ascent trajectory for maximum propulsion efficiency and insertion into orbit (Fig. 2); cruise vehicles which fly at lower Mach numbers but for longer periods of time; and rocket-powered space transports which fly a lower dynamic pressure ascent trajectory. Although the National Aero-Space Plane sees the maximum loading intensities, a hypersonic cruise vehicle could, depending on the mission, be subjected to a larger total heat load. The effect of the flight envelope and the propulsion system is related to Design Driver 5: for cruise, structural mass fraction affects range and/or payload, but for space transportation systems it affects the payload to the extent that it can eliminate mission considerations.

Airframe Structures

Concepts. Figure 3 shows the three basic types of airframe structures. The simplest approach conceptually is a hot structure that accommodates the aerodynamic heating. This type of structure was used on the SR-71/YF-12 and the X-15 aircraft. Although the advantage of such an approach is its simplicity, the disadvantages are that most materials that can be used at elevated temperatures (such as superalloys) are heavy, the outer surface must be relatively smooth, and thermal stresses which are difficult to predict can be relatively high. Thus, there has not been much work on such concepts since the review by Heldenfels[2] at the 5th ICAS Meeting in 1966. However, developments in metal matrix composites and higher temperature titaniums may make this approach more attractive.

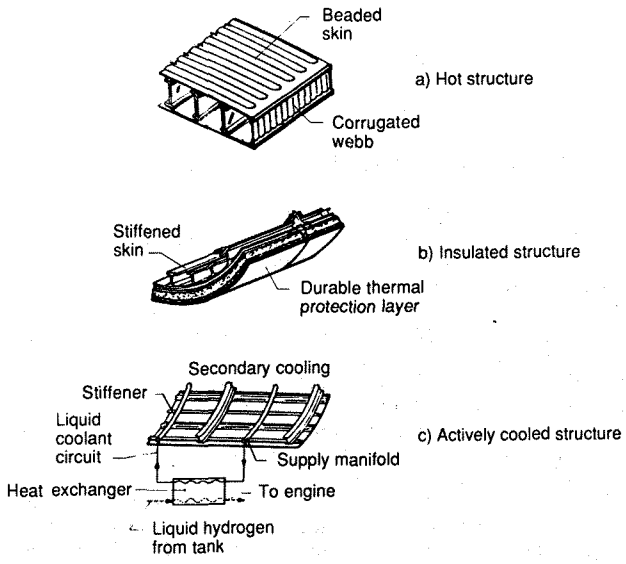

Figure 3. Typical airframe structural concepts.

A more complex approach is to use a more structurally efficient material and protect it from high temperatures by use of thermal protection systems (TPS). This is the approach that was taken for the U.S. Space Shuttle Orbiter where rigid and flexible ceramics have been used for the TPS that protect the aluminum primary structure. The most complex approach, proposed by Becker[21], is an actively cooled structure where the fuel, such as hydrogen or a secondary coolant such as water-glycol, is passed through tubes or cooling passages to convect the heat away from the structure. Because of the lack of interest in hypersonic cruise, where active cooling is most likely to be used for airframe structure, there has been little work done since Kelly[9] presented the status for this type of structures at the 11th ICAS Meeting in 1978.

Primary structure. One advantage of insulated structures is that the primary structure does not have to have a smooth external surface and thus it can be more structurally efficient. For a structural panel to have maximum geometric efficiency, the principal load-bearing area (caps) should be symmetrical about the neutral axis, have a high local buckling coefficient (curved caps and clamped edges), have a low-density web between the caps (low-core density), and have its core material supporting load. The three panel geometries shown in Figure 4 have improved geometries from left to right. The tubular panel satisfies three of these factors, but not the low-core density. The beaded web corrugation does not have a load-bearing core whereas the truss-core web corrugation satisfies all four geometry efficiency factors. Experimental results were in good agreement with structural analysis for the first two panel types. The truss-core web configuration is the subject of current design and fabrication research.

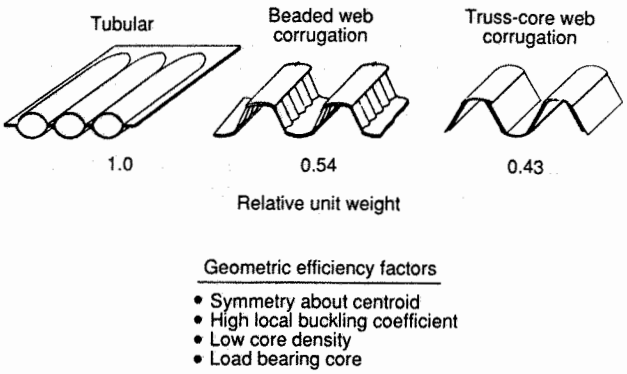

Figure 4. Geometrically efficient structural panels.

Such concepts offer significant weight savings and, if they can be fabricated from the advanced materials that are just now emerging, revolutionary reductions in structural mass fraction are a distinct possibility.

Control Surfaces. A concept design study has been conducted to determine a feasible design for a control surface for NASP. Both actively- and passively-cooled concepts were investigated. The most promising concept is shown in Figure 5 and is the lightest weight concept of all those considered. Although several factors were used in evaluating the concepts, weight was considered the single most important factor. The selected control surface design consists of two rib-stiffened carbon-carbon panels attached together and to a carbon-carbon torque tube support frame. Issues that must be resolved in the development program include high-temperature fasteners, characterization of carbon-carbon material, design of rib-stiffened panels, design and fabrication of the torque tube, design and fabrication of the torque tube-lug attachment joint, and attachment of the rib-stiffened panels to the torque tube. The difference in the thermal coefficients of expansion between the carbon-carbon torque tube and the superalloy lug fittings must be accounted for in the attachment design.

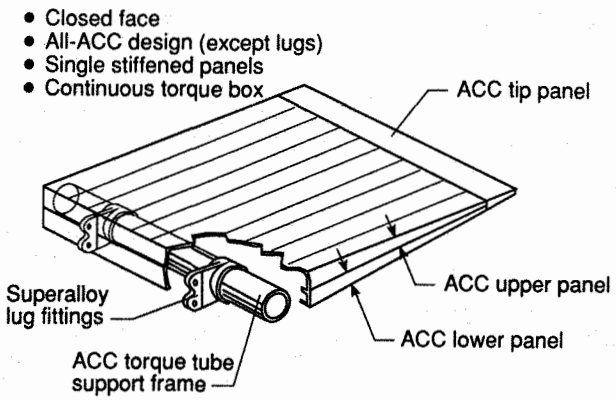

Figure 5. Control surface concept.

Leading Edge/Nose Cap. The U.S. Space Shuttle Orbiter uses carbon-carbon for both the nose cap and leading edge designs which has performed reasonably well to date. However, for longer duration cruise applications or for air-breathing single-stage-to-orbit (NASP) vehicles, the total heat load and/or maximum heating will require alternate approaches. One approach is shown in Figure 6. The design philosophy of this concept utilizes the high specific strength of carbon-carbon at elevated temperatures to accommodate the thermal/structural loads, and very thin refractory-metal D-shaped, heat pipes, embedded within the structure to transport the stagnation heat aft, where it can be rejected by radiation. The heat pipes could be sized and spaced close enough so that, in the event of a failure, the ablation protection afforded by the carbon-carbon would be sufficient to enable a safe reentry. The preferred method of construction would be to fabricate, fill, and checkout the individual heat pipes, embed them in a 2-D layup of carbon-carbon prepreg and process (pyrolize and densify) as you would a typical carbon-carbon component. 2-D thermal/structural analysis indicates the feasibility of the concept. Reaction rate studies of refractory metals, (molybdenum, tungsten, and tantalum), indicate that tungsten is the least reactive with carbon, and because of its very high thermal conductivity and low coefficient of thermal expansion, it is the leading candidate for a container for the lithium working fluid. Tungsten tubes have been successfully embedded within 2-D carbon-carbon prepreg, pyrolyzed and densified three times without any noticeable damage to the composite. Actively-cooled concepts such as back side convective cooling and mass addition cooling are also under study for those areas where the heating is most severe.

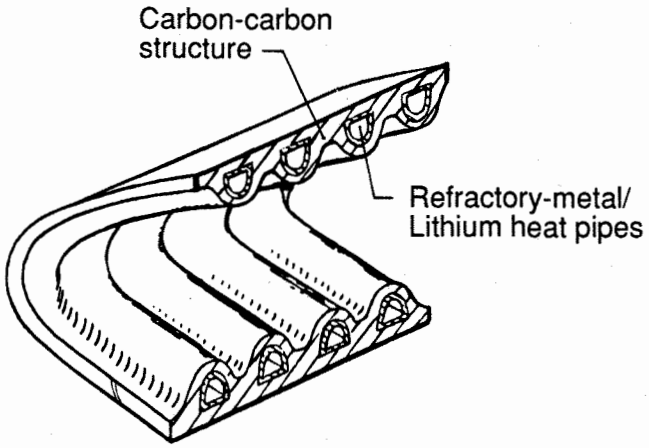

Figure 6. Carbon-carbon/refractory-metal heat-pipe leading edge concept.

Cryogenic Tanks

Concepts. Since reusable launch systems and hypersonic transports will become virtual flying cryogenic tanks, the design of such structure will dominate the airframe structures effort for such vehicles. The primary problem, which distinguishes hydrogen tanks from other cryogenic tanks, is the proclivity of liquid hydrogen to condense other gases because of its extremely low temperature (-423°F). Air, or any purge gas other than helium, condenses on the tank surface and produces a partial vacuum which pumps additional gas to the surface where it is condensed. This cryopumping (as it is called) transmits large quantities of heat to the fuel causing hydrogen boiloff and, if the gas is air, produces a potential safety hazard because of the selective liquefaction of oxygen from the air. No large, flightweight, reusable cryogenic tank has ever been flown; in fact only one has ever been built. The tank was a double-bubble (lobed) nonintegral half-scale (6000 gal.) tank. It was subjected to limited testing and no combined loads (thermal and structural) tests were conducted. A variety of hydrogen tank concepts have been proposed in conceptual studies in the past, however, the technology for such concepts has received little attention, and none of the concepts have been proven completely acceptable for multiple reuse applications. Thus cryogenic tanks are one of the key and least developed technologies for reusable hypersonic vehicles.

Tank Structure. The only existing reusable Space Transportation System (STS), the Space Shuttle, employs an aluminum expendable external cryogenic fuel tank, but future systems designed for full reusability will undoubtedly carry their

own cryogenic fuels internally. Consequently, structural design of fully reusable systems must necessarily address problems associated with containment of cryogenic fuel as well as the conventional considerations of thermal protection and support of vehicle structural loads.

Figure 7 gives two generic wall constructions for a section of cryogenic tank that cover the range from the most simple to most complex arrangements. The simplest concept is a honeycomb structure that 1) contains the cryogen and acts as a cryogenic insulation, i.e., low conductivity through the thickness, 2) carries the body loads, and 3) absorbs the aerodynamic heating and resultant thermal stresses. The low conductivity desired for reduced heat to the cryogen leads to undesirable thermal gradients which increase the thermal stresses that must be accommodated. The Boeing Aerospace Company has studied such a concept (Fig. 8) for a low-wing loading, sled-assisted takeoff single-stage-to-orbit vehicle. Boeing proposed titanium honeycomb sandwich for the upper surface which sees temperatures of about 600°F, and Rene' 41 for the lower surface which sees temperatures of about 1400°F.

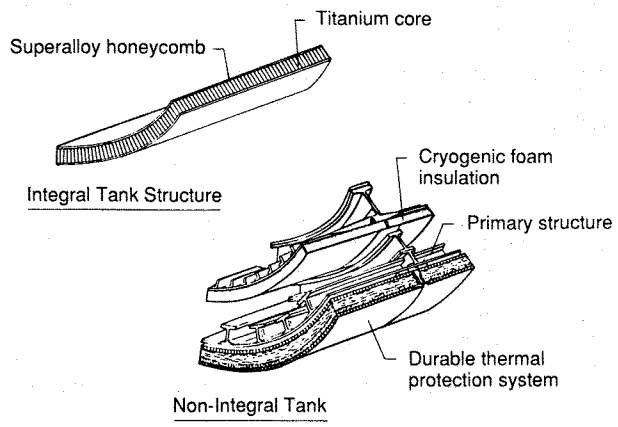

Figure 7. Integral and nonintegral creep tank/structure/TPS concept.

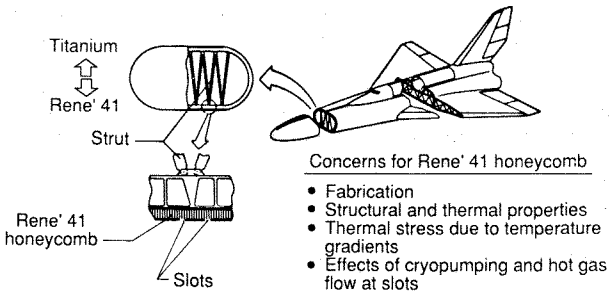

Figure 8. Integral tank/fuselage hot-structure concept.

Such a concept is obviously limited by the maximum use temperature of available structural materials. A material with a better specific strength and/or stiffness, and lower operating temperature, may be competitive with the "hot" integral structure approach if a thermal protection system (TPS) is used to reduce the heat load to the structure. The most complex approach (Fig. 7) is to have a tank to contain the cryogen, structure to carry the primary structural loads, and a TPS to reduce the heating to the interior structures. In addition, this approach has a cryogenic insulation (foam) to reduce boil off of the cryogen. Of course, the combined weight of the tank, structure, and TPS must be less than the weight of the hot honeycomb structure to be weight competitive. In addition, the TPS must provide the durable surface required for adverse weather flight and the complete system must be amenable to quick inspection, repair and recertification.

The honeycomb structure (Fig. 7) consists of a vacuum-sealed-cell honeycomb sandwich with the inner skin of the fuselage at a temperature of -423°F due to exposure to the cryogenic fuel and the outer skin at a temperature of 400°F due to exposure to the boost aerothermal environment. These temperature gradients produce large thermal stresses which must be accommodated in the design. The thermal stresses have been partially relieved by slotting the outer face sheet on the windward surface of the vehicle fuselage. These slots eliminate biaxial compression stress which would otherwise occur from thermal and pressure loads. The slots are sized to be nearly closed when the outer surface of the panel is heated to 1400°F. Pressure loads in the noncircular section are carried by tension struts at each frame location.

A Rene' 41 honeycomb panel, 1-ft. by 6-ft., was tested under combined thermal and bending loads at the NASA Dryden Flight Research Facility. The purpose of these tests was to evaluate the life of a panel when exposed to cyclic combined thermal and mechanical stresses. The panel was exposed to 500 boost cycles and 500 entry cycles. For each cycle, the mechanical load was held constant while the thermal load was applied. The maximum compressive strains were up to 80 percent of the proportional limit. After the first entry cycle, a small bow in the panel in the longitudinal direction was observed. This residual bowing gradually increased with additional exposure to entry cycles, but it was unaffected by additional boost cycles. No damage occurred as a result of the 500 boost and entry cycles, but the panel was left with a permanent center displacement of 0.58 in. over the length of 6 ft. with the concave face on the hot side.

A 21x25-in. panel was fabricated with several slots in the outer skin and tested to evaluate the effects of the slots in the boost environment. The panel formed the bottom of a container which was partially filled with LH_2. Hold times between cycles ranged from 10 min. to 1 hr. during which cryodeposits accumulated on the panel surface and in the slots. The panel was inspected after cycle 10 and cycle 30, and no damage to the panel was observed. After 36 cycles, a fire occurred in the test fixture but caused no damage to the panel. The panel was examined visually and by X-ray and C-scan. Sections cut from the panel were examined by metallographic inspection. No structural damage was found.

During the hold times, water frost was observed depositing on the -200°F panel surface, and temperatures less than -300°F measured during the tests indicated that liquid air formed in the regions of the core open to the atmosphere. These results indicate that proper attention must be given to sealing honeycomb core splices to prevent passage of air into the core from the slots. Without such sealing, considerable liquid oxygen may condense within the honeycomb structure. Additional details are given in Ref. 22.

Cryogenic Insulation. The most advanced cryogenic insulations for reusable LH_2 and LOX tanks are closed cell foams. Work on subsonic applications suggested reuse at temperatures up to 175°F. Calculations indicate that a substantial savings in insulation thickness (and hence, weight) can be achieved if the maximum use temperature can be increased to 400°F or higher. Most recent work in this area has been focused on developing a system for 400°F applications with a goal of 500 thermal-cycle life.

The foam system under study consists of 40-inch-square tiles which contain 16 ten-inch-square blocks of Rohacell SF110 grade foam adhesively bonded together. The 40-inch-square tile is encapsulated within a Kapton-Aluminium-Kapton (KAK) cover to minimize permeation of gases. These tiles are in turn bonded to the surface of the cryogenic tank and the joints between the individual tiles are sealed with another layer of KAK over the joints. A 10-inch-square tile has been fabricated and tested as an exterior insulation. The thermal structural

loading represents the loads on a high-speed aircraft LH_2 tank. The specimen has been tested for 25 cycles at LH_2 temperatures and 225 cycles at LOX temperatures with no apparent degradation of the cryogenic insulation function. Future tests are proposed using lower density foams and larger tile arrays with joints. Also tests are planned to determine the conductivity, permeability, and compatibility of the various Rohacell foams in partial pressure environments that simulate the actual anticipated use condition for the foam systems.

For air-breathing SSTO vehicles a lighter system may be required. Current concepts of interest are evacuated foil gage titanium honeycomb or multiwall panels and multilayer insulations. The main challenges are maintaining a vacuum with foil material, sealing of joints, and long life foil material for encapsulating the multilayer insulation.

TPS. Although the Reusable Surface Insulation (RSI) currently used on the Space Shuttle is an excellent insulation, it may not be durable enough for commercial transport and second generation space transport applications. Thus, the Langley Research Center has a program to develop more durable TPS using metallic concepts for temperatures from 700°F to 2000°F and using Advanced Carbon-Carbon (ACC) above 2000°F. The goals of the program are to develop TPS that have durable surfaces, are mechanically attached, have covered gaps between panels to reduce gap heating, and are mass competitive with current systems.

Two metallic TPS concepts are shown in more detail in Figure 9. The two metallic prepackaged concepts are discrete panels that have a strip of RTV-covered felt beneath the perimeter of each panel to prevent hot gas flow beneath the panels. The titanium multiwall concept (maximum surface temperature <1200°F) consists of layers of dimpled titanium foil Liquid Interface Diffusion (LID)® bonded together at the dimples with a flat foil sheet sandwiched between each dimpled sheet. The superalloy honeycomb concept (maximum surface temperature <2000°F) consists of an Inconel 617 honeycomb outer surface panel, layered fibrous insulation, and a titanium honeycomb inner surface panel. The edges of the two metallic concepts are covered with beaded closures to form discrete panels nominally 12 inches square.

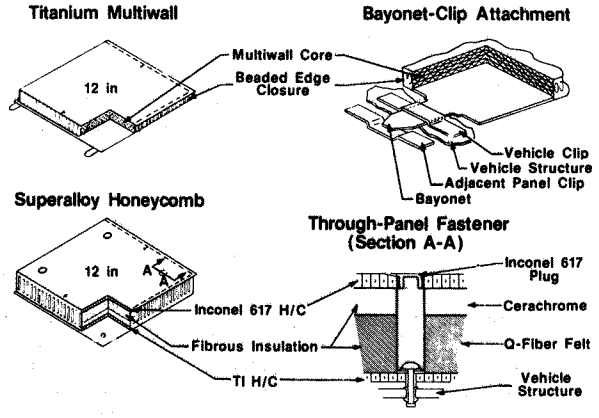

Figure 9. Metallic TPS concepts.

The two types of attachments shown in Figure 9 can be applied to either of the TPS concepts. The bayonet-clip attachment, shown with the titanium multiwall concept, consists of two clips and a metal tab (bayonet) LID bonded to the lower surface of the panel. One clip is mechanically attached to the vehicle surface, and one clip is LID bonded to the lower surface of an adjacent panel. Thus, a single bayonet attaches a corner from each of two adjacent panels. The through panel fastener, shown with the superalloy honeycomb concept, consists of a thin-walled cylinder through the panel that allows access to a bolt which fastens the panel corner to the vehicle structure. The cylinder, which contains fibrous insulation, is covered with an Inconel 617 threaded plug.

NASA test facilities at Johnson Space Center (JSC), Kennedy Space Center (KSC), and Langley Research Center (LaRC) were used for verification tests of the concepts. TPS test models were exposed to combined temperature and pressure conditions to obtain thermal response characteristics of the concepts using thermal/vacuum test facilities at JSC, KSC, and LaRC. Dynamic response of metallic TPS concepts was evaluated by shaker-table vibration tests and by acoustic exposure in a sound chamber at JSC and a progressive wave facility at LaRC. The acoustic levels were representative of those experienced during Space Shuttle lift-off. Environmental tests to assess water retention and the effects of atmospheric contamination on metallic TPS are being conducted near the Space Shuttle launch site at KSC. Additional water retention tests were conducted with a wind/rain machine at JSC. Lightning strike tests, were conducted at LaRC to determine how much damage lightning impact caused on the metallic panels. The metallic TPS concepts were tested in the LaRC 8-Foot High Temperature Tunnel (8' HTT) to evaluate the performance of the concepts in an aerothermal environment. Details of these investigations, which indicated good structural and thermal performances, are given in Ref. 23.

Engine Structure

Concepts. One of the greatest challenges of air-breathing hypersonic flight is the design of the hydrogen fueled scramjet engines for the vehicles. Because of the high density and total enthalpy of the air flow, heating of the exposed structure can be extreme - combustor heating rates may exceed 2000 BTU/sq.ft.-sec. These heating levels require the use of active cooling systems to maintain the engine structures at survivable temperatures. One method of active cooling is to use surface heat exchangers (cooling jackets) attached to the exposed engine walls with the hydrogen fuel as the coolant. There are many different cooling jacket designs, but two that have been previously investigated are the channel fin and pin fin cooling jackets. Schematics of the channel fin and pin fin geometries are shown in Figure 10 along with the cross section of a conceptual two-dimensional scramjet engine. The major components of the scramjet engine are the inlet, combustor, and nozzle. Three basic engine shell structural concepts have been investigated: two frame-stiffened honeycomb-core sandwich panels and a deep core honeycomb sandwich panel. All three concepts have approximately the same mass per unit capture area. The deep-core honeycomb concept exhibits the least deflection in the sidewall and nozzle areas and is the least complex structure. Analytical results indicate relative displacements between adjoining components are generally small which permit the panel corners to be rigidly joined allowing the use of a simple static seal or even a welded corner. The results indicate that the basic shell concepts have a significant temperature gradient through the thickness during thermal transients (e.g., maneuvers, combustion shutdown) which may significantly impact the final design of both the seals and basic shell structure.

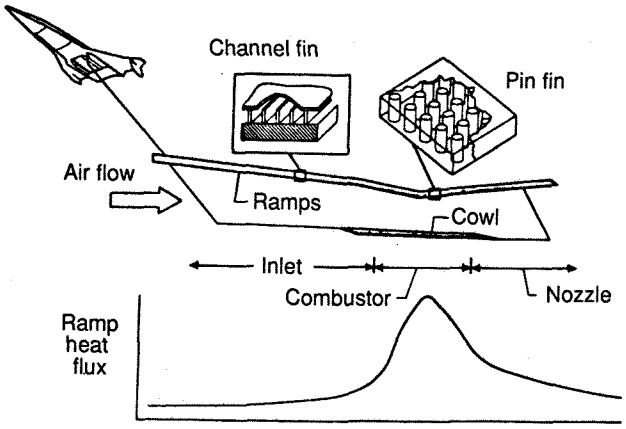

Figure 10. Scramjet engine schematic with cooling jackets.

Engine Walls. A heat-pipe sandwich panel was conceived (Ref. 24) as a simple and efficient solution to the engine wall thermal stress problem. The heat-pipe concept can drastically reduce maximum temperature differences across the honeycomb walls, and, hence, reduce thermal stresses with only a modest increase in mass (less than 10%) over the original, unacceptable nonheat-pipe design. This exceptional performance is possible because the integral heat-pipe sandwich panels synergistically combine the thermal efficiency of heat pipes with the structural efficiency of honeycomb sandwich construction. Several panels were fabricated and tested to verify feasibility of the concept. The goal was to develop a sandwich panel, similar in structural integrity to the original nonheat-pipe sandwich panel design, which could reduce maximum temperature differences, hence, stresses, by 50% and make the design feasible.

The heat-pipe sandwich panel consists of a wickable honeycomb core, internally wickable facesheets, and a suitable working fluid. The term "wickable" is defined as porous and capable of wicking a working fluid by capillary pumping. For application to the scramjet engine, the working fluids considered were cesium, potassium, and sodium. During operation, heat is absorbed at the heated face by the evaporation of working fluid. The heated vapor flows due to a pressure differential, to the cooler face where it condenses and gives up its stored heat. The cycle is completed with the return flow of liquid condensate back to the heated face by the capillary pumping action of the wickable core. The core is perforated to allow intracellular vapor flow and is notched at both ends to allow intracellular liquid flow along the internally wicked faces.

The heat-pipe sandwich panel test specimens were 6x6x1 in. and were manufactured from stainless steel to reduce costs. For actual engine application the panels would be fabricated from a high-temperature superalloy. The facesheets were made internally wickable by sintering one layer of 120x120 mesh screen to 0.024-in.-thick sheet material. Two different types of wickable core were considered: 165x1400 mesh woven wire screen (0.0055-in. thick) and screen/foil composite, 325x325 mesh screen (0.0025-in. thick) sintered to 0.003-in.-thick foil. The entire sandwich panel is fabricated by simultaneously spot welding the core ribbons to each other and to the facesheets, forming a 0.375-in. cell configuration. This all-welded manufacturing technique eliminates concern for materials compatability problems of the working fluid with a bonding agent.

The sandwich panels were radiantly heated by quartz lamps to simulate the scramjet engine startup transient. Two panels, one empty and the other filled with working fluid, were tested simultaneously. The panels were subjected to the same heating environment; heat was applied over one surface of the panels (the top surface) while the other surface and sides of the panel were insulated to simulate adiabatic boundary conditions. Models were instrumented with thermocouples to monitor heat-pipe startup and performance and to determine maximum through-the-thickness (face-to-face) temperature differences.

Results of the tests indicate that the heat-pipe sandwich panels with sodium working fluid were capable of reducing maximum temperature differences by 31% over a nonheat-pipe sandwich panel, by 46% using potassium as the working fluid, and by over 60% using cesium as the working fluid. Comparison of temperature difference histories of a cesium filled heat-pipe panel and a nonheat-pipe panel are shown in Figure 11. As shown, the temperature differences of the front and back facesheets of both panels coincide up to about 300°F. At this point, the heat-pipe panel begins to operate and reduces the temperature difference. The reduction in maximum temperature difference for this test is 60%. Hence, it appears that the heat-pipe sandwich panel concept can meet the goal of a 50% reduction in temperature differences and therefore is a promising solution for alleviating thermal stresses in a scramjet engine while resulting in only a 10% increase in mass over the original, unacceptable design.

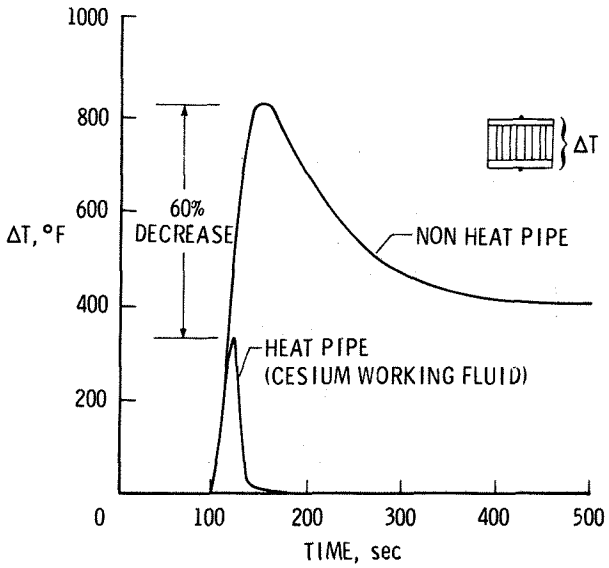

Figure 11. Comparison of face sheet temperature difference histories.

Although the technology developed to date for engine walls provides a good data base for a Mach 6 to 10 cruise vehicle, the structural concepts are too heavy to be considered for an air-breathing SSTO space plane. In addition, if the heating environment becomes much more severe, backside convective cooling cannot absorb enough of the heat load to keep structural temperatures within reasonable bounds. Thus advanced materials and mass addition cooling (either film or transpiration) are required for such a mission.

Strut. A major effort, which is nearing completion, has been a contracted activity with Allied Signal (Garrett-Airesearch) for the design and fabrication of a flightweight fuel injection scramjet strut as outlined in Figure 12. Major challenges result from the environment and functional requirements imposed on this structural component. Cryogenic hydrogen enters through an inlet manifold, provides impingement cooling along the stagnation line of the leading edge, flows back through a pin-fin cooling jacket along both surfaces of the unsymmetrical body, and returns to the engine as fuel. The fuel enters another manifold and is injected through two rows of ports on one side, one row on the opposite side, and a row along the trailing edge. The 2-foot span, 48°-swept leading edge component was designed

such that the Inconel 718 primary structure would be fabricated in two parts with forward and aft sections formed with sheet metal technology for more economical fabrication. Machined Inconel support beams and leading edge section, and the chemically-etched Nickel 201 pin-fin external cooling jacket are attached in a two-step brazing process. To allow for inter-mediate fabrication verification (e.g., pressure checking) a 0.01-in. face sheet is brazed to the pin fins prior to brazing the jacket to the primary structure. Many fabrication problems were identified and resolved. The last and most vexing problem concerned braze management in attaching the cooling jacket to the primary structure - too much braze material resulted in blockage at the forward and aft ends and too little braze resulted in braze voids as shown in the photograph of a preliminary short strut fabrication (Fig. 13). Since "fit-up" is the key to successful brazing of flat surfaces, a series of 0.005-in. grooves has been provided in the face sheet. This reduces the stiffness of the cooling jacket (better fit-up) and also the grooves provide access for any excess braze. Specimen tests have shown that this, in combination with hot sizing, provides good braze results. Final assembly and brazing of the full length strut are imminent. Functional testing in a flow environment with fuel burning is planned in a test cell at the Langley Research Center.

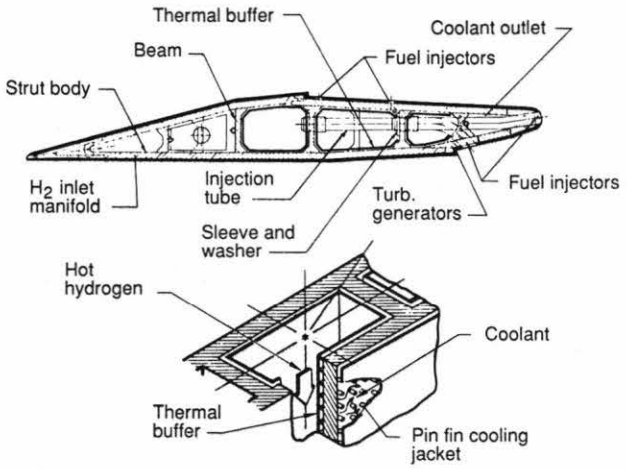

Figure 12. Fuel injection scramjet strut.

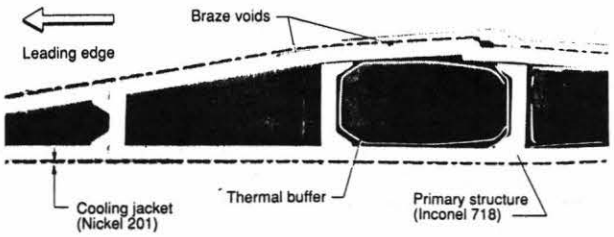

Figure 13. Cross-section of short strut.

Cowl Lip. The incident shock generated by the vehicle nose or compression ramps on the undersurface of a vehicle acts to precompress the air flow passing into the engine as illustrated in Figure 14. Aerodynamicists' design for this shock-on-lip condition to maximize the compressed air flow into the engine and hence performance. The shock wave interference problem illustrated is a formidable thermal-structural design issue for hypersonic vehicles with air-breathing engines. The experimental configuration in the lower left of Figure 14, which simulates the vehicle forebody and cowl leading edge, was used to define the aerothermal loads. The schlieren photograph shows a supersonic jet interference pattern impinging on the surface of the cylinder. The interference pattern produces intense local amplification of the pressure and heat transfer in the vicinity of the jet impingement. The undisturbed (absence of incident shock) stagnation point pressure and heating rate can be amplified by factors from 6 to 30 depending on the shock strength and free stream Mach number.

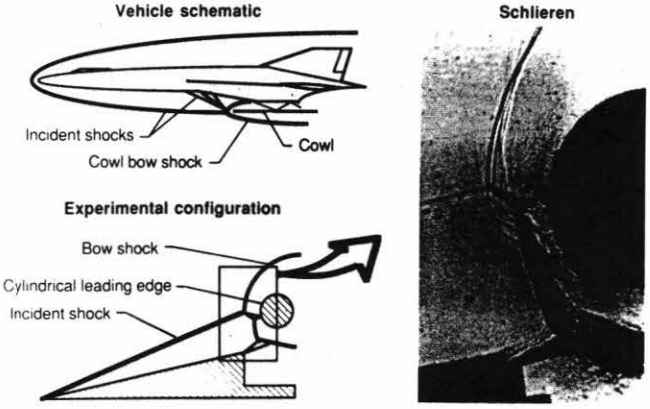

Figure 14. Shock-on-lip interference phenomena.

These experimental data were used to calibrate finite element solutions and adaptive meshing techniques for the flow field and surface pressures and heating rates. The adaptive unstructured grid techniques performed well as illustrated in Figure 15. Additional details of this effort are given in Ref. 25.

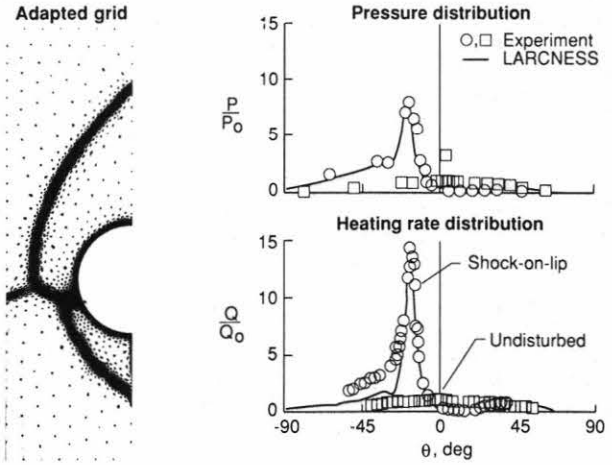

Figure 15. Comparison of analysis with experiment.

Parametric 2-D studies have been conducted to investigate potential solutions for cowl lip designs subjected to such severe heating. Figure 16 shows results from two such studies (Refs. 26-27). One study, shown in the lower left of the figure, looked at the advantages of adding high-conductivity graphite fibers to tungsten to reduce the circumferential temperature gradients resulting from the intense local heating of the shock-shock interaction. Both the maximum temperature and temperature gradient were reduced, but lateral stresses along the leading edge are still severe. Thus plastic strains and limited cycle life are concerns.

The Langley Integrated Fluid Thermal Structural (LIFTS) analyzer (Ref. 26) was used to investigate the benefits of internal fins and thermal superconducting materials for reducing thermal gradients and stresses by increasing the thermal energy absorption by the hydrogen coolant and increasing circumferential diffusion. LIFTS predicts the external heating and structural heat transfer to the coolant using finite element methods. A 0.25-inch-diameter leading edge is subjected to

transient shock-wave interference heating typical of acceleration through Mach 16 which causes the vehicle nose bow shock to sweep across the engine cowl leading edge from an outboard to an inboard position, which creates the shock-on-lip interference pattern shown in the upper left figure. The interference heating rate reaches a peak value of 30,000 BTU/ft^2 sec. at about 22° below the horizontal centerline of the leading edge. The inner surface is convectively cooled by the direct impingement of the sonic hydrogen jet stream with an inlet temperature of 50°R and pressure of 1000 psia. Internal tapered fins around the circumference of the leading edge increase the effective convection area by a factor of 2.5. The physical area is increased five times, but because the fins are not isothermal the fin efficiency factor is 50%. Copper and beryllium are the candidate thermal superconducting materials because they provide significantly higher thermal conductivity than nickel, the baseline unfinned concept. The peaks of the thermal conductivity for copper and beryllium, which occur at 20°R and 70°R, are approximately 300 and 80 times higher than the nickel, respectively, as shown in the upper right of Figure 16.

The peak temperature, where the shock interference occurs, was reduced from 2500°R for the nickel to 1000°R for the beryllium, and to 766°R for the copper as shown in the lower right figure. The circumferential temperature gradient was also reduced significantly, but still results in an axial stress level about 100 ksi even for the copper. Since this stress level exceeds the material elastic limits, the design is cycle-life limited. Thus additional studies are required to determine a design with an acceptable life.

III. Materials

Lightweight high-temperature materials development is an enabling technology for reusable hypersonic vehicles. The specific strength and stiffness of leading candidate materials[28] for NASP are shown in Figure 17. For temperatures up to 1600-1800°F RSR titanium, titanium-aluminide intermetallics, and fiber-reinforced versions of these alloys are being developed as part of the NASP program.[29] These materials are preferred over superalloys because of their lower density and potentially higher specific properties. For temperatures in excess of 1800°F, carbon-carbon and ceramic matrix composites are the most structurally efficient materials. The timely development of these materials for light weight hot structures which will be repeatedly exposed to severe hypersonic flight conditions is a very formidable challenge requiring significant advancements on several fronts. New developments in Al alloy technology for hypersonic applications include weldable Al-Li alloys for cryogenic tanks and high-temperature Al for reusable flyback boosters. The key issues and highlights of ongoing research on the major material systems being currently considered for future hypersonic vehicles will be discussed in the following sections.

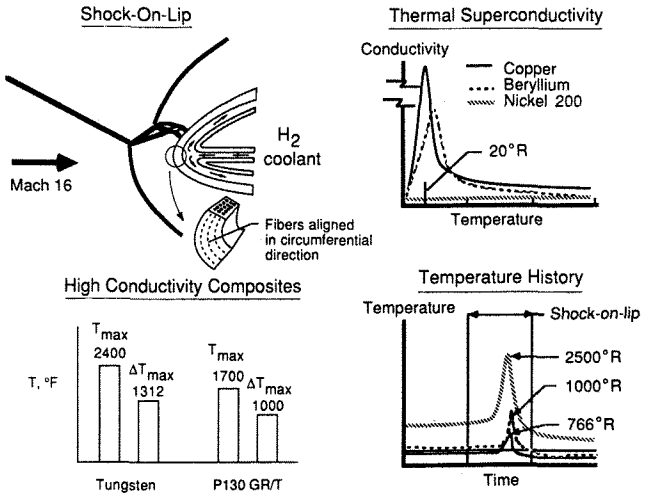

Figure 16. H_2 impingement-cooled leading edge results.

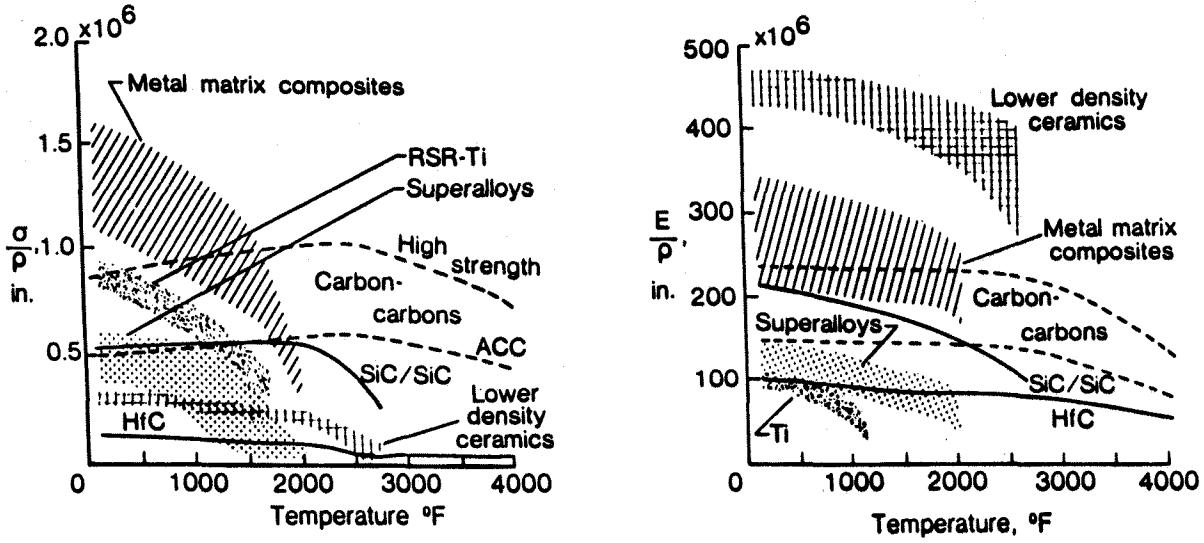

Figure 17. Candidate materials for hypersonic applications.

Metals and Metal-Matrix Composites

Superalloys. Superalloys have been successfully developed and used in jet engines for hundreds of hours in the 1400-2000°F temperature range. In general, superalloys have excellent oxidation resistance and good microstructural stability. Although almost all of the work on superalloys was directed at turbine engine applications, a small but significant amount of work was performed by NASA during the late 60's and early 70's for supersonic and hypersonic transport airframe structures, and the thermal protection systems for shuttle. A representative indication of the types of test articles fabricated are the heat shield concepts shown in Figure 9. A significant data base was generated on the mechanical and physical properties of sheet gage materials made from a number of different superalloys. The effect of sheet thickness on creep resistance of selected superalloys at 1400°F is shown in Figure 18. For both Rene' 41 and Haynes 188 alloys at 1400°F the 0.010-inch sheet had a markedly lower creep resistance than the 0.020-inch sheet. For the Rene' 41 alloy the difference was an order of magnitude. These results are particularly important because they illustrate that data generated on sheet material may not be very useful for predicting the lifetimes of very thin gage alloys being considered for some of the new lightweight structural concepts.

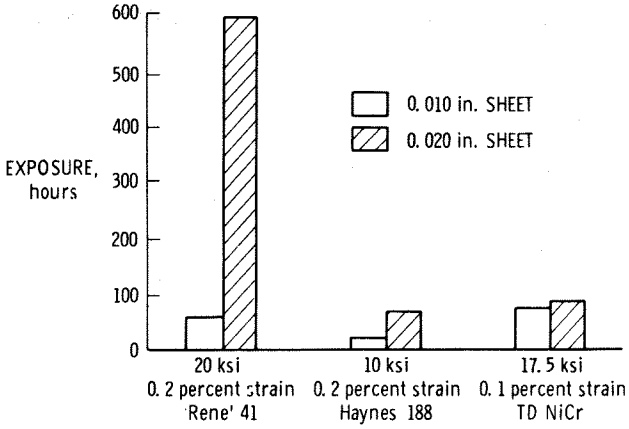

Figure 18. Effect of sheet thickness on creep resistance.

An example[30] of the type of data generated on the oxidation behavior of superalloys after 100 hours of cumulative exposure at 1800°F is shown in Figure 19. Both continuous and half-hour cyclic exposures were conducted on 0.020-in.-thick sheet material. The oxidation resistance of TD-NiCr (Thoria dispersion strengthened NiCr alloy) was far superior to that of the other two superalloys examined.

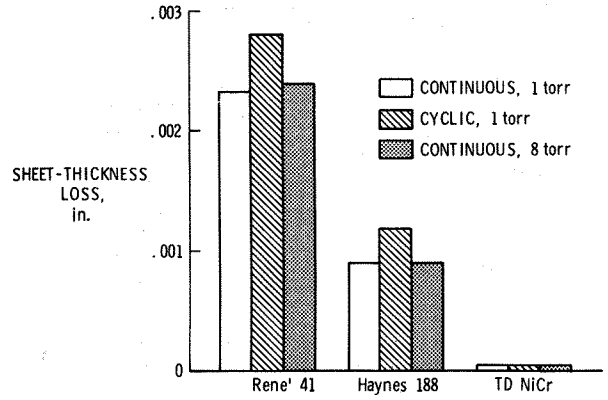

Figure 19. Superalloy sheet-thickness loss.

For a given reentry environment the surface temperature is governed primarily by the emittance and catalytic activity of the surface. Good progress in lowering the catalytic activity of superalloys for heat shield applications has recently been reported[31]. Data for Inconel 617 and a dispersion-strengthened iron base superalloy MA-956 are shown in Figure 20. The borosilicate coatings applied to the surface in a thickness of a few hundred angstroms resulted in a dramatic reduction in the catalytic activity of the MA-956 surface resulting in a 600°F decrease in the equilibrium surface temperature for the particular exposure conditions selected for this test. Research on these and similar coatings is continuing and arc-jet tests for realistic size panels are planned to verify results obtained on small 1-inch-diameter disk specimens.

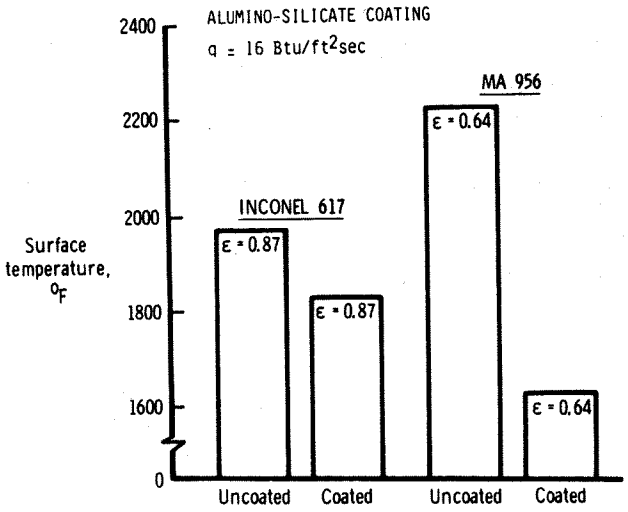

Figure 20. Effects of coatings on catalysis of superalloys.

Ordered Alloys and Metal-Matrix Composites. Long-range-ordered alloys are a unique new class of high-temperature structural alloys. The relatively slow atomic mobility and unique dislocation dynamics in ordered lattices result in these alloys having unusual properties such as the yield strength increasing rather than decreasing with increasing temperature.[32] The creep and fatigue strengths of these alloys at elevated temperatures are generally superior to similar disordered alloys. However, these alloys tend to be brittle at room temperature. Recent alloy development work performed at Oak Ridge National Laboratory has produced a number of long-range-ordered alloys $(Fe,Ni)_3V$, $(Fe,Co,Ni)_3V$, $(Fe, Co)_3V$ which have good ductility.[33] Although Fe, Ni, and Co-base intermetallics look very attractive for many high-temperature applications, they are generally considered to be too heavy for weight-critical hypersonic vehicles like NASP. The NASP materials program has focused on the development of titanium aluminides and titanium aluminide composites because they offer the greatest potential for meeting mission requirements. Representative properties[34] of some aluminide materials are compared with those of conventional titanium and nickel-based alloys in Table I. Titanium aluminide has a density approximately half that of superalloys with a stiffness 50 percent greater than that of titanium alloys. The modulus of conventional titanium alloys drops rapidly with temperature to a value of approximately 10 Msi at 1000°F whereas TiAl has a higher modulus at 1832°F than titanium does at room temperature. The creep strength of the aluminides is very good as is the oxidation resistance, particularly TiAl, which is an alumina former. The most significant limitation on the aluminides is their low ductility at room temperature.

Table I. Properties of high-temperature alloys.

	Ti Base	Ti_3Al	TiAl	Superalloys
Density (lb/in^3)	.163	.150 -.170	.136	.300
Young's Modulus (Msi)	16 -14	21-16	25	30
Max. Temp. - Creep (°F)	1000	1500	1900	2000
Max. Temp. - Oxidation (°F)	1100	1200	1900	2000
Ductility - R.T. (%)	~20	2-5	1-2	3-5
Ductility - Operating (%)	High	5-8	7-12	10-20

For programs such as NASP where the ultimate in performance is demanded from the materials, fiber reinforcement of titanium aluminide alloys is a key materials development activity. Projected rule of mixture properties of conceptually possible titanium aluminide metal-matrix composites[35] are shown in Table II. There is a significant increase in specific strength in going from Rene' 41 to Ti_3Al; however, there are much larger benefits in specific strength and specific stiffness when comparing isotropic materials to the metal-matrix composite lamina. The optimum fiber and matrix combination for a particular application is strongly influenced by the type of loads to be carried. For strength-critical applications the IM6 graphite fiber might be considered whereas for stiffness-critical applications P100 graphite fibers would be the preferred choice. However, before graphite-reinforced titanium alloys can become a practical reality, coatings must be developed to prevent fiber/matrix interactions. The ability to uniformly coat thousands of individual graphite fibers with a thin yet protective high-temperature coating is a formidable technology challenge.

Table II. Specific strength and stiffness properties calculated from rule of mixtures .

MATERIALS	E. MSI	ULT.KSI	ρ. #/IN^3	E/ρ. IN.	ULT/ρ. IN.
Rene' 41	31.6	170	.298	106 x 10^6	570 x 10^3
Ti_3Al	20	180	.180	111	1000
P100/Ti_3Al(1)	57.5	240	.130	442	1850
IM6/Ti_3Al(1)	32	440	.128	250	3440
SiC/Ti_3Al(1)	41	315	.141	291	2230
TiB_2/TiAl(1)	37.5	295	.159	236	1860
TiB_2/Ti_3Al(1)	35	315	.180	194	1750
TiC/TiAl(1)	44.5	295	.166	268	1780
TiC/Ti_3Al(1)	42	315	.187	225	1680

(1) • Room temperature, elastic, unidirectional
• Rule of mixtures for strength and stiffness
• Maximum fiber strain for strength
• 5% weight penalty for fiber coating
• 50% fiber volume

Fiber diameter is an important consideration for minimum gage applications where cross-ply laminates are required to carry biaxial loads. The highest strength SiC fibers commercially available are approximately .0056 in. in diameter which means that three-ply composite laminates of SiC/Ti_3Al could not be fabricated less than .020 inch. There is a pressing need for small-diameter high-temperature fibers which are chemically compatible with titanium-base alloys for very long periods of time at temperatures up to 1600-1800°F.

An important consideration in the development of metal-matrix composites (MMC) is understanding how damage develops and the sequence of events which lead to failure. Depending on the relative fatigue behavior of the fiber and matrix, and the interface properties, the failure modes in MMC can be grouped into four categories: 1) matrix dominated, 2) fiber dominated, 3) self-similar damage growth, and 4) fiber/matrix interface failure. Fiber/matrix separation is most likely to occur in MMC systems with high-yield strength matrices which causes high load transfer between fiber and matrix in the off-axis plies. This type of failure mode has been observed in SiC/Ti-15-3 composites[36] as illustrated by the photomicrographs shown in Figure 21 and the stress-strain curves shown in Figure 22. Figure 21 shows the general fracture surface of a $[0/\pm45/90]_S$ laminate.The presence of essentially bare SiC fibers on the fracture surface suggests weak bonding between the fibers and matrix. The presence of a reaction zone on individual fibers such as the one shown in Figure 21 indicates that the weakest interface may be between the base alloy and the fiber/matrix reaction zone. Tensile stress-strain curves of these laminates were nonlinear with a knee at approximately 20 ksi, well below the matrix materials minimum yield strength of 100 ksi. In all cases, the unloading elastic modulus was less than the initial elastic modulus, thus indicating that some sort of damage had occurred in the laminate. A typical loading and unloading curve of a $[90]_8$ laminate after the first ten cycles is shown in Figure 22. The unloading curve closely followed the loading curve indicating an opening and closing phenomenon. Fiber matrix separation during loading was confirmed by an edge-replica technique which indicated that the fiber matrix interface opened upon loading and closed when the specimen was unloaded.

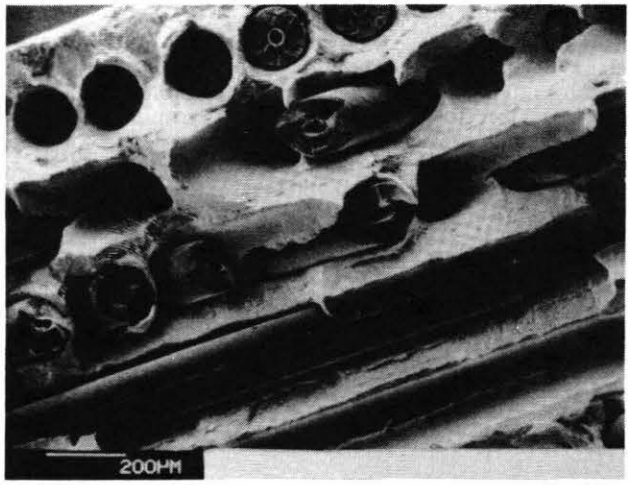

Overview of fracture surface

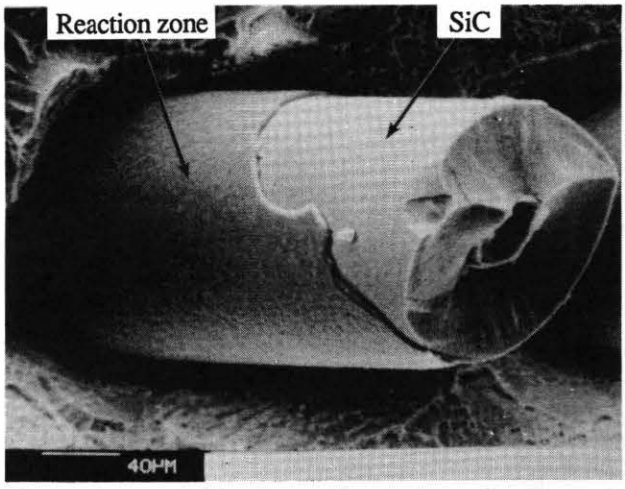

Debonded fiber surface.

Figure 21. Fracture surface of SiC/Ti-15-3.

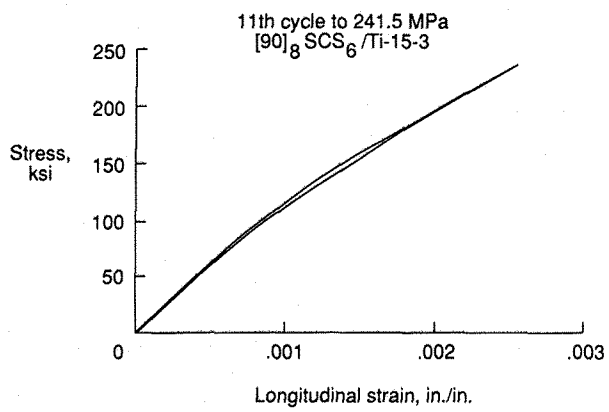

Figure 22. Stress-strain response of SiC/Ti-15-3.

Recent tests[37] have shown that a weak fiber matrix interface can significantly affect the fatigue response of silicon-carbide fiber-reinforced titanium matrix composites. S-N data were experimentally determined for four different layups containing 0° plies. The stress-strain response was monitored during the fatigue life. The stiffness dropped very early in the cycling history due to fiber/matrix interface separations. Fatigue cracks in the matrix, such as those which form in B/Al, were not observed in this materials system. After a few cycles the stiffness stabilized and the cyclic strain range was recorded. This stabilized strain range was multiplied by the fiber modulus (60 msi) to determine the cyclic stress range in the fiber. The number of cycles to failure was then plotted against the cyclic stress in the 0° fibers. The fatigue data from the four different laminates were correlated very well by the 0° fiber stress as shown in Figure 23.

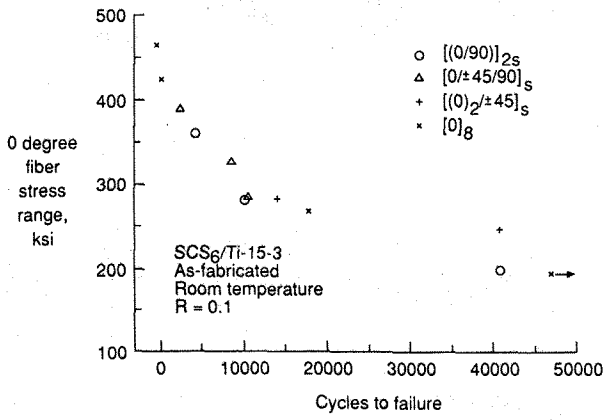

Figure 23. Cyclic stress range of SiC/Ti-15-3.

It is important to note that fiber failures were not the first damage to occur in these composites. The first damage that caused significant modulus change was the failure of the fiber/matrix interface in the off-axis plies. However, increasing the strength of the fiber matrix interface bond may reduce both the fatigue life and fracture toughness because of self-similar crack growth. The strain to the matrix fatigue limit is close to the fiber failure strain. Since the fatigue limit is significantly lower than the yield stress, the matrix may develop fatigue cracks without yielding the matrix globally. Furthermore, high stress concentration can be created in titanium alloys in a fiber ahead of a matrix crack. The net result of these factors can be self-similar crack growth and lower fracture toughness in well bonded Ti MMC. Much additional work is required to understand failure modes and approaches to improve strength and toughness of Ti-based MMC.

Aluminum Alloys. New developments in aluminum alloys, Figure 24, which could improve the performance of hypersonic vehicles are the development of aluminum-lithium-based alloys and high-temperature aluminum alloys. Commercial alloys containing Al-Li-Cu-Zr (e.g., 2090) and Al-Li-Cu-Mg-Zr (e.g., 8090) are becoming available[38-39], particularly for fastened airframe components. Current research on these alloys is addressing issues associated with low fracture toughness, mixed-mode fatigue crack growth, environmental stability, and heterogeneous microstructure. Studies are also underway to add minor alloying constituents to improve the weldability of these alloys and eliminate the requirement to do a cold stretch before aging to achieve maximum strength. Recent results[40] have shown that minor additions of indium to the Al-Li-Cu-Zr system change the precipitation characteristics of the alloy such that cold deformation before aging is not required. This is potentially very significant because it means that superplastic forming could be used to fabricate complex structural elements, and the elements then heat treated. Recent progress has also been made in the development of a new Al-Li alloy which is weldable[41], has excellent strength, good fracture toughness, and cold work is not necessary to achieve maximum strength.

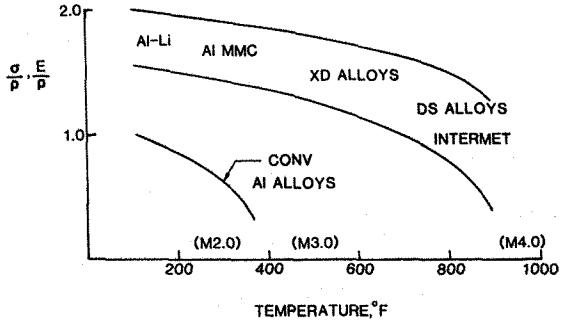

Figure 24. High-temperature aluminum-based alloy systems.

High-temperature Al alloys are also being considered for reusable launch vehicles. Several new alloy compositions (based on Al-Fe-V-Si, Al-Fe-Ce, Al-Fe-Mo, etc. systems) have been developed[42-44] which offer significantly higher mechanical properties at elevated temperatures than conventional 2000 and 7000 series Al alloys traditionally used for airframe applications. These alloys could be very attractive for reusable launch vehicles, because higher temperature capability of the airframe structure would require less thermal protection to resist aerodynamic heating.

Fabrication Technology. A recent study[45] was conducted at NASA Langley to develop joining and fabrication processes to facilitate the efficient incorporation of Ti_XAl into lightweight, high-temperature honeycomb sandwich structure. Ingot metallurgy (I/M) Ti-14A1-21Nb was selected as the face sheet material due to availability and its chemical composition which approximates that of some of the RSR Ti_XAl alloys currently being developed. Ti-3A1-2.5V honeycomb core was the only titanium alloy honeycomb core commercially available.

The fabrication processes which were selected based on their potential for fabricating a minimum weight, high-temperature sandwich structure were brazing, Liquid Interface Diffusion (LID®) bonding[46], and Enhanced Diffusion Bonding (EDB).

Enhanced Diffusion Bonding is a term used to define the joining process being investigated at the NASA Langley Research Center for joining titanium base alloys.[45] A typical layout for an EDB Ti-14A1-21Nb face sheet, Ti-3A1-2.5V honeycomb sandwich panel is shown in Figure 25. The panel components consist of two face sheets joined to the honeycomb by means of EDB. The honeycomb core is electroplated with

copper on the edges of the core only. The assembled panel components are heated in vacuum to the bonding temperature and held at temperature for a sufficient period of time to promote interdiffusion of the EDB material at the core-to-face-sheet interface to establish a eutectic[47] composition. As a result, a liquid phase is created. As further diffusion occurs and the composition of the liquid changes, the melt solidifies. Thus, the remelt temperature of the EDB joint is higher than the original joining temperature. Potential advantages of the process compared to brazing include less filler metal required due to higher joint strengths and higher joint remelt temperatures. Compared to diffusion bonding, less bonding pressure is required and joint fit-up tolerances are less critical due to the formation of a liquid phase.

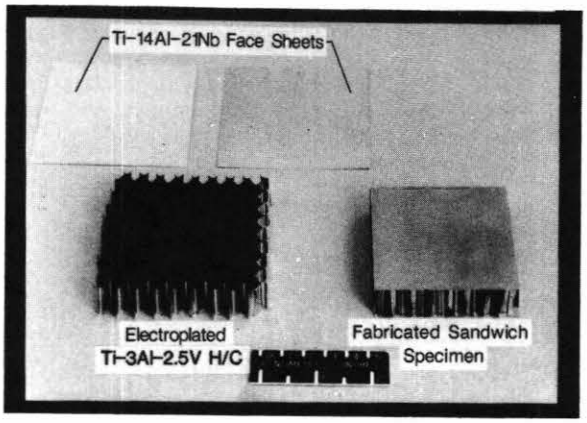

Figure 25. Honeycomb-core sandwich components and fabricated specimen.

A photomicrograph of a typical joint segment of an EDB honeycomb sandwich panel in which the copper EDB material was selectively plated only on the edge of the honeycomb core is shown in Figure 26. A very small fillet of copper EDB material has formed at the joint interface and the eutectic liquid has fully diffused into the face sheet to a depth of only 0.001 inch. In addition, there was no visible EDB copper material on the core walls and the transformed microstructure extended only 0.005-in. up the core walls. This photomicrograph shows that localized application of the copper EDB material using a selective removal of maskant plating technique minimizes both the weight penalty and the deleterious interaction effects associated with the materials required for joining. It is estimated that less than five percent of the face sheet area was affected by the EDB process.

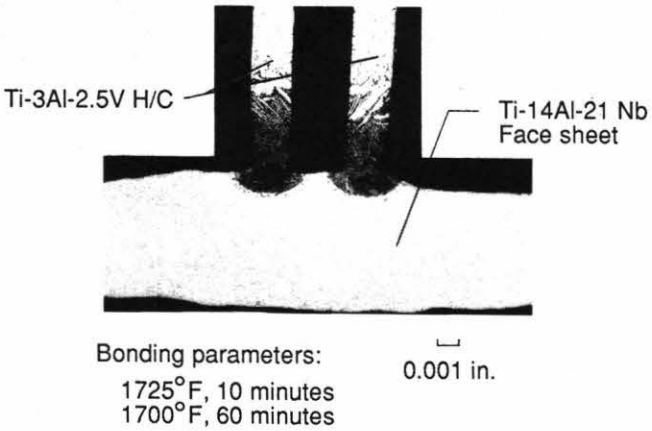

Figure 26. Microstructure of face sheet/honeycomb-core interface.

The flatwise tension strength of EDB Ti-14A1-2Nb face sheet honeycomb core coupon specimens is plotted in Figure 27 along with aluminum brazed Ti-6A1-4V face sheet honeycomb core coupon data.[48] The EDB coupon data should be comparable with the aluminum brazed data since the alloy, foil thickness and cell configuration of the honeycomb core are the same. The flatwise tension strength of the EDB specimens is one-fourth that of the aluminum brazed specimens at room temperature but is approximately equal at 1000 and 1100°F. The difference in the strength below 400°F is attributed to the larger quantity of braze alloy used in the aluminum brazing process which substantially increases the load-carrying capability of the honeycomb core. At the higher temperatures of 800-1100°F, the strength contribution of the aluminum braze is substantially reduced and the failure loads of the two sandwich types are nearly equivalent. The difference in the flatwise tension strength of the EDB specimens fabricated with 0.020-inch and 0.007-inch-thick face sheets is attributed to differences in the face sheet surface finish and variations in the amount of copper required for EDB.

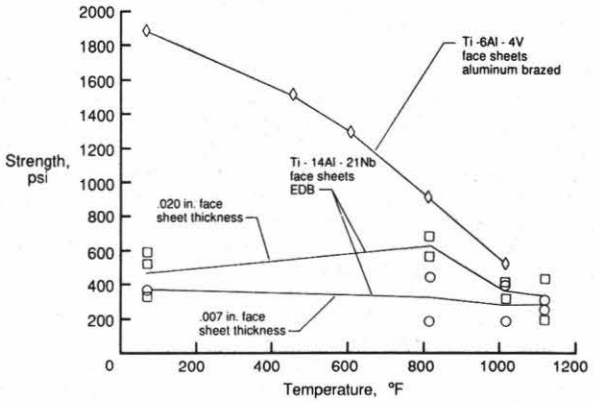

Figure 27. Flatwise tension strength of honeycomb-core sandwich specimens.

Environmental Effects. An extensive amount of work will be required to identify damage mechanisms and to develop a fundamental understanding of the environmental durability of candidate materials for hypersonic vehicles. Materials used on hypersonic vehicles will be subjected to extremely hostile environmental conditions. These may include hot hydrogen, high-temperature oxidation, transient thermal and pressure loads, low- and high-cycle fatigue, impact damage, and corrosion. Two of the most pressing issues currently being worked as part of the NASP program are hydrogen embrittlement and high-temperature oxidation. Materials on reusable hypersonic vehicles could see an extremely varied series of hydrogen environments, ranging from liquid hydrogen at cryogenic temperatures and low pressures to gaseous hydrogen at extremely high temperatures and high pressures.

The liquid hydrogen storage tank is expected to experience hydrogen temperatures from about -400°F to the maximum temperature allowed for the tank structure and hydrogen pressures to about 50 psi. Times at these conditions could be on the order of hundreds of hours at cryogenic temperatures, thousands of hours at room temperature, and tens of hours at the maximum allowable temperature. Repeated cycling between these conditions will occur.

The fuel lines and valves are expected to experience the entire spectrum of anticipated conditions, with hydrogen temperatures ranging from -400°F to about 2000°F and hydrogen pressures ranging from a few psi to thousands of psi. Times at these conditions could be long with numerous thermal and pressure cycles.

The actively-cooled areas of the engine and airframe are anticipated to see temperatures and pressures similar to those described above for the plumbing. Time at elevated temperature is expected to be several minutes, with hundreds of cycles to atmospheric pressure and room temperature. Additionally, the rate of heating and cooling of these components could be quite rapid.

Although hydrogen degradation of monolithic metallic materials has been extensively studied[49], very little basic information is available on either the hydrogen interaction or hydrogen transport (diffusion and permeation) processes in titanium-aluminide systems. The limited work that has been performed has been devoted to characterizing the isothermal gaseous hydrogen absorption characteristics of these materials. Based on very limited investigations, it appears that hydrogen solubility increases as the Ti/Al ratio increases. Under the conditions investigated to date, hydride formation is much more likely to occur in Ti_3Al than in TiAl.

Hydrogen barrier coatings may be needed to prevent hydrogen from being transported to vital structures of a hypersonic vehicle. Two types of barrier coatings, diffusion barrier coatings and noncatalytic coatings, can be considered. The former slows hydrogen entrance by slowing hydrogen diffusion and the latter slows absorption by reducing the rate of molecular hydrogen dissociation. However, past experience with barrier coatings[50] has shown them to be susceptible to damage during assembly, operation, and testing of components, and their service life is known to be affected by thermal cycling, temperature gradients, and microstructural modifications over time. Additionally, it is difficult to inspect a surface coating to insure even its initial integrity as a barrier.

The use of diffusion barrier coatings to protect against structural degradation appears reasonable at the lower temperatures, but not at elevated temperatures. Hydrogen transport is so rapid in most materials at temperatures approaching 2000°F that coating thicknesses become significant and minor defects in the coating will permit rapid local hydrogen entrance. A diffusion barrier coating also makes it difficult for hydrogen to exit a material once it enters. Noncatalytic coatings are thought to offer the greatest potential as hydrogen barriers because their effectiveness is generally not dependent on coating thickness.

Another environmental issue which is receiving considerable attention for hypersonic vehicles is high-temperature oxidation. There are two key issues: the first has to do with oxidation of the material, and the second is the need for the surface to have a high emittance and low catalysis. The oxide scale which forms on most metallic materials is catalytic and has a relatively low emittance (<0.8). Therefore, protective coatings that shield the materials from oxidation and have a low catalytic efficiency can significantly extend the applicability of metallic materials by reducing the heating rate to the surfaces in hypersonic flight environments that contain dissociated gas species. High-emittance coatings will reduce the temperature of hot structures by radiating a significant portion of the aerothermal heat flux away from the surface. A recent study[51] on the static and dynamic oxidation behavior of Ti_xAl alloys has been completed. A number of high-emittance, low-catalysis, oxidation-resistant coatings were exposed to dynamic oxidation in a simulated hypersonic environment. Static oxidation tests were conducted in laboratory air for times ranging from 25 to 120 hours and temperatures ranging from 1200°F to 2000°F using a thermogravimetric analysis apparatus. Samples were exposed to dynamic oxidation conditions for up to 5 hours at a surface temperature of 1800°F in the NASA Langley Hypersonic Materials Environmental Test System (HYMETS) facility (hypersonic flow conditions in this constricted arc heater were defined relative to flight envelopes[52]). Post-test evaluations on specimens included Arrhenius' analysis of the oxidation weight change data to determine kinetics data, radiative properties measurements to determine emittance, heating rate analyses to determine surface catalysis, and metallurgical evaluation to determine oxide phases and microstructural changes.

A total of three alloys with coatings comprising 26 alloy-coating combinations were evaluated. On the basis of pre-screening and short-time HYMETS testing, nine alloy-coating systems were suitable for 5 hours HYMETS evaluation. To this point, the 5-hour tests on the Ti-14Al-19Nb-8Mo samples have been completed. All the "successful" coatings have been thick "glass-like" layers that may experience mechanical failure (i.e., cracking, spalling, etc.) when applied to larger areas. Thick coatings also represent a significant weight penalty for a full-size vehicle.

The total normal emittance of three uncoated alloys (Ti-14Al-2Nb, Ti-34Al-1.5V, and Ti-14Al-19Nb-8Mo) and three coatings on Ti-14Al-19Nb-8Mo are shown in Figure 28. The three coatings (a pack aluminide with a sputtered SiO_2/pyrex coating; a double coating with one layer of pack silicide and one layer of pack aluminide; and a slurry glass/$MoSi_2$ coating) had emittances that were greater than 0.8 before and after dynamic oxidation testing.

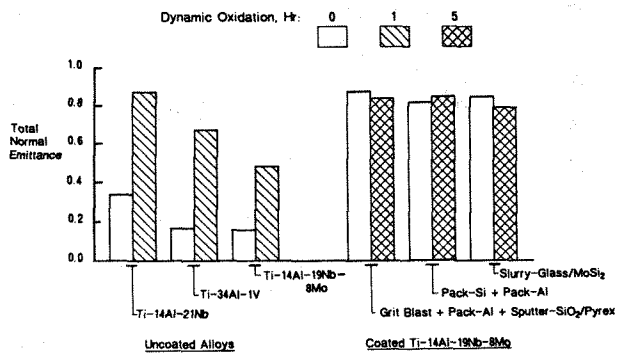

Figure 28. Total normal emittance at 1800°F.

The catalytic efficiencies of samples under steady-state heating conditions were determined by using the aerothermal heating to the sample and Goulard's solution[53] to the stagnation laminar flow heating equation. For hot structures at hypersonic flight conditions, these data are more important than the room-temperature catalytic efficiencies.

Figure 29 shows a comparison of catalytic efficiencies at 1800°F for a number of materials; data for the RCG Shuttle Tile Coating and the CVD boro-alumino-silicate coating are shown for reference. The efficiency of the RCG coating is in the range of metal oxides. The catalytic efficiency of Ti-14Al-19Nb-8Mo was much lower than that of Ti-14Al-21Nb. The efficiency of the Pack Si + Pack Al was quite high. Efficiencies for the Al + sputtered SiO_2 /Pyrex and slurry glass/$MoSi_2$ agreed well with those for the CVD coating.

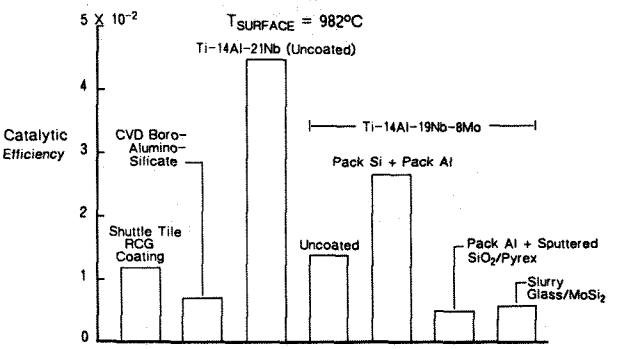

Figure 29. Comparison of catalytic efficiency at steady-state conditions.

Continuing research centers on two goals: the development of coating/substrate systems, and the characterization of material response through environmental testing. Consideration will be given to hydrogen permeability as well as emittance, catalysis, and dynamic oxidation.

Carbon-Carbon Composites

Applications. Carbon-carbon composites (C-C) are attractive candidate materials for thermal protection systems and hot structures for advanced hypersonic vehicles because of their light weight and good strength retention at high temperatures. The specific strength comparisons made in Figure 17 showed that above approximately 1500°F, carbon-carbon composites have the highest specific strength of any structural material. However, carbon oxidizes rapidly in air at temperatures above about 1000°F. Hence, applications for carbon-carbon composites must either be restricted to nonoxidizing environments, to short exposure times (minutes), or the composites must be protected from oxidation. To date, the only reusable oxidation-resistant C-C (ORCC) composite that has been developed and placed into flight service is that which is used as the thermal protection system (TPS) on the nose cap and wing leading edges of the Space Shuttle Orbiter[54]. Since this ORCC composite is used as TPS material rather than as primary structure, it need have only relatively modest mechanical properties. Because of the significant potential benefits to be obtained in employing C-C composites as hot structure, however, research is currently being pursued to develop improved methods of oxidation protection suitable for high-strength, high-modulus C-C composites [55-56]

The major steps in the fabrication of carbon-carbon composites[57] are shown in Figure 30. General performance requirements for selected applications of long-life, reusable ORCC composites are shown in Table III. The TPS material on Space Shuttle, designated Reinforced Carbon-Carbon (RCC) by its developer, Vought Corporation[58], is the only one demonstrated in service. Two additional applications of considerable interest are ORCC composites for man-rated turbine engines and for hot structural material on advanced aerospace vehicles. For man-rated turbine engines, target operational temperatures and hot lifetimes are 2500°F and 4000 hours [56], respectively. On advanced aerospace vehicles, materials requirements are expected to be more demanding than on Space Shuttle, as indicated.

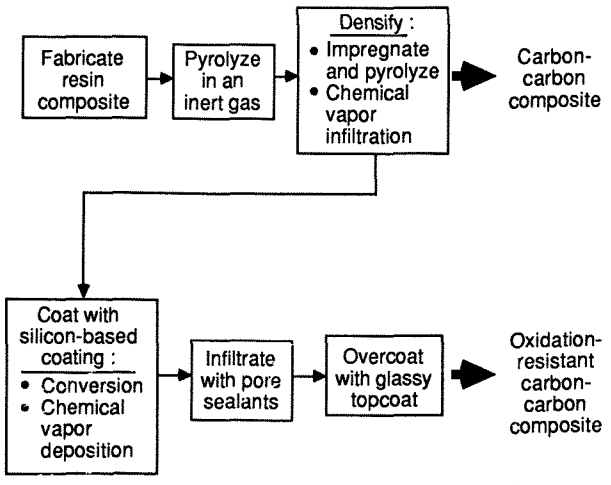

Figure 30. Carbon-carbon composite fabrication process.

Table III. Performance requirements of carbon-carbon composites.

	Space Shuttle nose cap and wing leading edges	Man-rated turbine engines	NASP airframe hot structure
Number of missions	100	Many	150
Hot lifetime, hrs	100	4000(b)	~ 250
Design temperature, °F	2700(a)	2500(b)	< 3000
Single-mission survivability temperature, °F	3000	-	> 3000
Operating environment	Air	Combustion products	Air
Operating pressure, atm	< 1	> 1	< 1
Mechanical property requirements	Low σ and E	High σ	High σ and E

(a) Actual flight experience 2500°F
(b) Air Force Technical Objective Document FY88, Dec 1986

Oxidation Protection. Reinforced Carbon-Carbon has been used very successfully on the nose cap and wing leading edges of the Space Shuttle Orbiter. Figure 31 shows thermal profiles for two locations on the wing leading edge during entry from orbit.[57] The stagnation area reaches the highest temperature. The lug attachment area reaches only a relatively low temperatures, but its mass loss is high because cracks are wider at these temperatures. The RCC oxidation protection system (OPS) consists of a SiC conversion coating, a tetraethyl orthosilicate (TEOS) crack sealer, and a proprietary overcoat sealer (Vought Corporation Type A). The OPS performs well at the 2500°F temperatures experienced in flight, but at higher temperatures decomposition and reactions of the OPS constituents, coating spallation, aerodynamic shear removal of low-viscosity sealants, and vaporization of sealants are expected to become problems. The lug attachment areas remain at relatively high temperatures after touchdown when the pressure has reached 1 atm. This severe oxidizing condition leads to a high oxidation mass loss. The high viscosity of the sealant at the lower temperatures in the lug area retards healing of cracks.

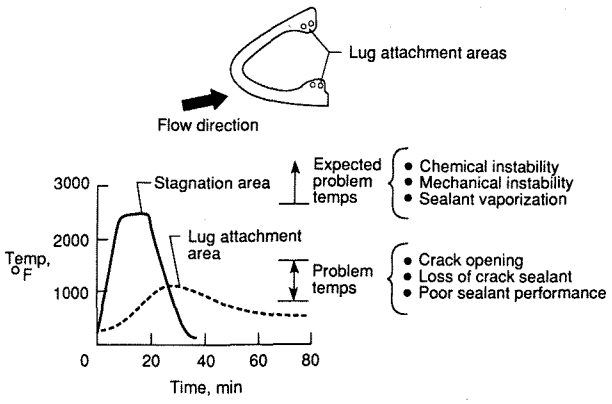

Figure 31. Space Shuttle Orbiter entry thermal profiles for wing leading edge.

Experimental data were needed in the Shuttle program to assess the effectiveness of the Shuttle baseline coating system and to predict the lifetime of the wing leading edge[59-60] Complete mission environments were simulated at both the stagnation and the lug attachment areas. These simulations included simultaneous application (in air) of load, temperature, and pressure on tensile.specimens. Testing was performed at NASA Langley in the Multiparameter Environmental Simulation Facility.

Early predictions of mass loss based on multiparameter test results indicated that the mass loss at the lug attachment area

would be excessive if baseline coatings were relied on exclusively for oxidation protection. Consequently, Type A sealant was developed and applied over the baseline coating to improve the oxidation protection. Figure 32 shows the improvement achieved in oxidation protection for five mission cycles when Type A sealant is used. The flight data shown in Figure 32 were obtained from 1/4-inch-diameter specimens which have been flown on all Shuttle missions. These specimens are removed and weighed after every five missions. The conclusion from these comparative data is that the multiparameter tests served as a good predictor of flight performance of RCC for the Shuttle environment.

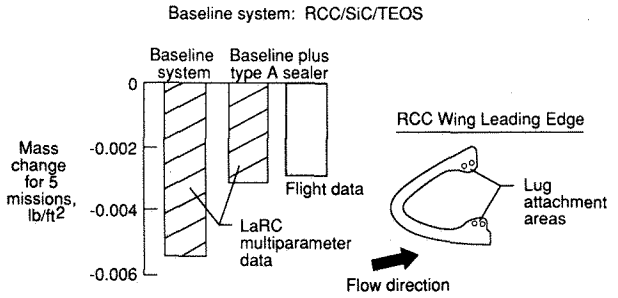

Figure 32. Oxidation of RCC.

Representative conditions of temperature and pressure for cruise and orbital vehicles[57] are depicted in Figure 33. These conditions are illustrative only, and not representative of any particular component. Clearly, precise conditions will depend on mission trajectory, Mach number, material surface properties (emittance, catalytic activity with respect to the recombination of dissociated boundary layer species), location on the vehicle, and other factors. There are certain general features of interest, however. Highest temperatures likely will be reached on ascent to and entry from orbit. These temperatures will be experienced for relatively brief periods of time and at low pressures. For cruise missions, peak temperatures will likely be much lower and there will be an extended period at intermediate temperatures. Cruise pressures will also be low, but not as low as those for orbit missions. Designing an OPS capable of successful operation in both types of environments poses a major technical challenge.

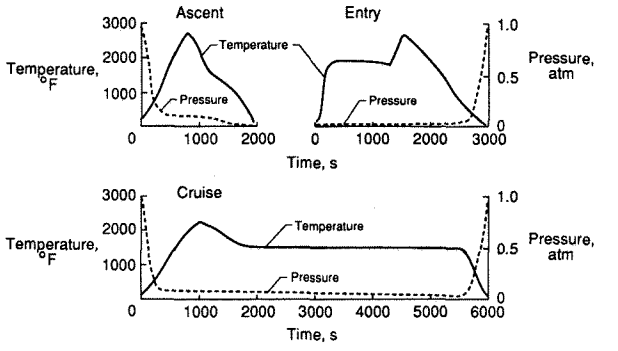

Figure 33. Representative service environments for carbon-carbon composites.

Many different oxidation-protection concepts have been explored. The basic features of these concepts are depicted schematically in Figure 34. The first line of defense against oxidation is the coating, typically SiC and sometimes Si_3N_4. Upon being exposed to high-temperature oxygen, these Si-based coatings form a very thin layer, or scale, of silica glass, which is a very effective diffusion barrier to oxygen and limits further attack. The maximum practical use temperature of these coatings is about 3000°F. Were it not for the fact that the coefficients of thermal expansion (CTE) of these coatings differ markedly from those of typical C-C substrates, such coatings would be all that is required for effective oxidation protection. Unfortunately, because of differences in CTE, cracks develop in these coatings upon thermal cycling, and oxygen can penetrate through these cracks to the substrate.

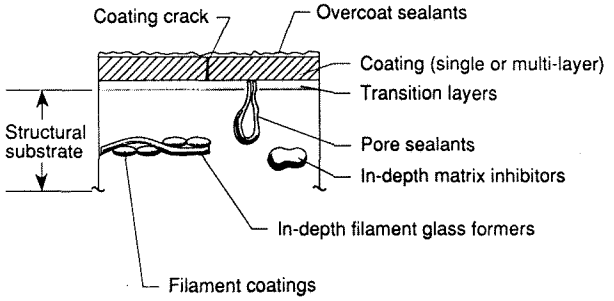

Figure 34. Oxidation-protection considerations.

The second line of defense against oxidation consists of various internal and overcoat glassy sealants used to block oxygen from reaching the substrate through these cracks. Typical sealants are based on silicate and borate glasses Sometimes the coatings themselves are multilayered with glasses or glass-formers in them, or transition layers of other materials are employed between the coating and the substrate to reduce the CTE incompatibility and to anchor the coating better to the substrate. A third line of defense against oxidation consists of various inhibitors added to the matrix. These inhibitors function both as oxygen getters and as glass formers. They typically consist of Si, B, Zr, and various compounds of these metals. Limited research has been conducted to incorporate inhibitors directly into the reinforcing fibers themselves[61], but this approach tends to weaken the fibers and has yet to be developed to any significant extent. In some cases, fiber coatings are also used.

Performance evaluations of selected ORCC materials are being conducted in Langley's Multiparameter Environment Simulators under environmental conditions similar to those depicted in Figure 33. Initial test results[57] for candidate materials have shown substantial mass loss upon initial exposure, followed by a period of fairly constant mass loss until about 31 hours cumulative exposure (11 entry plus 7 cruise cycles). After this point, the loss rate increased for entry cycles but remained relatively unchanged for the cruise cycles. The initial large mass loss may be attributed to vaporization of some constituent from the glass sealant system. Microscopic examination of the specimen surface following each exposure revealed what appeared to be a continual migration of glassy material to the surface of the specimen, with the formation of bubbles. The region of steady mass loss can be due to continual loss of sealant, oxidation of carbon from the substrate, or a combination of both.

Following these oxidation exposures, specimens were sectioned and examined microscopically. Separation of the coating from the substrate was noted at some locations, while similar but less severe delaminations were also noted on both faces of the specimen at several other locations. Separation of the coating from the substrate may have been caused by internal gas pressure generated by volatilization of sealant and inhibitor constituents. The CTE mismatch between the coating and substrate may have been a major contributor. Since the maximum test temperature for the specimen is presumed to be higher than the coating deposition temperature, the coating would be in compression at these maximum temperatures. Since the coating in the OPS basically floats on a liquid layer of glass at high temperatures, there are no significant shear or interlaminar forces to resist an upward buckling of the expanding coating. In support of this position is the fact that the observed distance of separation between the coating and substrate is consistent with the distance calculated using the CTE data.

Substrate Development. If carbon-carbon composites are to be used for primary airframe structures the strength properties need to be increased. Following the Shuttle technology development program, NASA sponsored research[62-64] to develop an improved carbon-carbon composite. The result was the development of "Advanced Carbon-Carbon" (ACC) which has approximately doubled the in-plane strength of RCC. Two approaches are currently being pursued to improve the interlaminar shear and interlaminar tensile properties of ACC. One approach is to improve matrix strength through process optimization. Key variables investigated have included matrix composition, fiber surface treatments, pyrolysis conditions, and reinforcement architecture. The results[65] of this approach have been only moderately successful to date. The second approach being pursued[66] is to use three-dimensional (3-D) reinforcement schemes where fibers strengthen through-thickness strengths. A schematic illustration of a 3-D fabric and integrally-stiffened panel is shown in Figure 35. A 3-D orthogonal weave material tested at Langley gave more than a three-fold increase in interlaminar shear strength, and more than a two-fold increase in interlaminar tensile strength compared to ACC. The flexure strength of the 3-D composites was also approximately 65 percent higher than 2-D ACC. The reason for the increase was related to a change in failure mode, from delamination in the 2-D material to fiber microbuckling in the 3-D material.

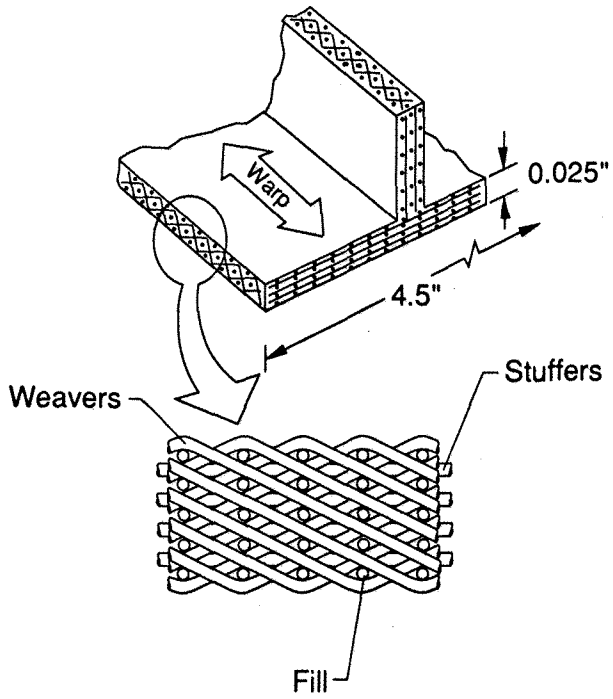

Figure 35. Integrally-stiffened carbon-carbon panel.

IV. Concluding Remarks

It has been shown that for hypersonic vehicles to provide the performance benefits desired, the structures and materials technical community has many challenging tasks. A myriad of concepts have been proposed over the last 30 years, but only a few were carried all the way to fabrication and testing. Improvements in structural performance are thus still possible and, in fact, probably required. However, the maximum payoff, and perhaps the enabling technology, is advancements in materials that have high specific strength and stiffness, thermal properties compatible with use in hot/cooled structural applications, and retention of ductility and fabricability required for efficient concepts with sufficient life under cyclic thermal loads.

Cryogenic tank development is an enabling structures technology as only one large, flightweight tank has ever been built and none has ever been flown. Even the question of how to certify for flight reusable cryotanks is currently taxing the engineering ingenuity of the participants in the U.S. National Aero-Space Plane (NASP) program. Leading edges with adequate life, particularly cowl lips for air-breathing space transports, are still an elusive goal requiring considerable innovative effort. Past work with superalloys has revealed the difficulty of fabricating some of the complex structures required for hypersonic vehicles, and has also revealed that the fabrication process can have a deleterious effect on the material properties and hence structural performance of the actual hardware. Additionally we have learned that data generated on sheet material may not be very useful for predicting the lifetimes of foil gage alloys which are being considered for some metallic TPS concepts.

Much remains to be done. Research in high payoff areas of materials and structures has barely scratched the surface. One of the most exciting areas is the development and use of advanced carbon-carbon materials for acreage TPS and structural applications. The major challenges in such applications are improved oxidation-resistant coatings and substrate strength properties. Another exciting area is the exploitation of ordered alloys and metal-matrix composites in high-temperature structural concepts. Ordered alloys have excellent creep and fatigue strengths at elevated temperatures. Unfortunately, they tend to be brittle at room temperature where the maximum mechanical loads are anticipated. The NASP program is currently focusing on titanium aluminides with and without fiber reinforcement. The most significant limitation on the aluminides is their low ductility at room temperature. Use of graphite fibers awaits the development of coatings that will prevent fiber/matrix interactions. High strength SiC fibers tend to avoid the fiber/matrix interaction, but their current size (.0056-in.- diameter) leads to heavy minimum-gage material or severely limits the advantages of structural tailoring. Thus, there is a pressing need for small diameter high-temperature fibers which are chemically compatible with titanium-based alloys for very long periods of time at elevated temperatures.

This paper has documented some of the progress in addressing the challenges of materials and structures for high-temperature applications to hypersonic vehicles. Significant progress has been made in some areas, very little in others. If hypersonic vehicles are to become a reality, a long-term focused technology development program must be supported.

V. References

1. Heldenfels, R. R.: Historical Perspectives on Thermostructural Research at the NACA Langley Aeronautical Laboratory from 1948 to 1958. NASA TM-83266, Feb. 1982.

2. Heldenfels, R. R.: Structural Prospects For Hypersonic Air Vehicles. Presented at the 5th Congress of the International Council of the Aeronautical Sciences (ICAS), London, England, Sept. 1966.

3. Norton, Allan: Test Set-Up and Equipment Description Report, Double Wall End Item. ASTESS-61-5, November 1961.

4. Norton, Allan: Boeing Hot Structure Phase II Test Program. ASTESS-62-1R, May 1962.

5. Grogan, John C.: Development Test Summary in Support of X-20 Elevon Structural Test Program. AFFDL-TR-65-191, January 1966.

6. England, Murray N.: X-20 Window Tests. AFFDL-TR-65-211, January 1966.

7. Hughes, Thomas F.: Thermantic Structure Test Program. AFFDL-TR-66-76, June 1966.

8. Monfort, John B.: Structure Test Program - Advanced Structural Concept Experimental Program (ASCEP). AFFDL-TR-70-8, August 1970.

9. Kelly, H. Neale; Wieting, Allan R.; Shore, Charles P.; and Nowak, Robert J: Recent Advances in Convectively Cooled Engine and Airframe Structures for Hypersonic Flight. Presented at the 11th Congress of the International Council of the Aeronautical Sciences (ICAS), Lisbon, Portugal, Sept. 1978.

10. Jones, Robert A.; and Huber, Paul W.: Airframe Integrated Propulsion System for Hypersonic Vehicles. Presented at the 11th Congress of the International Council of the Aeronautical Sciences (ICAS), Lisbon, Portugal, Sept. 1978.

11. Kelly, H. N.; Rummler, D. R.; and Jackson, L. R.: Research in Structures and Materials for Future Space Transportation Systems -- An Overview. J. Spacecraft and Rockets, vol. 20, no. 1, Jan.-Feb. 1983, pp. 89-96.

12. Kelly, H. Neale; and Gardner, James E.; Compilers: Advances in TPS and Structures for Space Transportation Systems. NASA CP 2315, Dec. 1983.

13. Howe, John T.: Introductory Aerothermodynamics of Advanced Space Transportation Systems. J. Spacecraft and Rockets, vol. 22, no. 1, Jan.-Feb 1985.

14. Martin, J. A.: Hydrocarbon Rocket Engines for Earth-to-Orbit Vehicles. J. Spacecraft and Rockets, vol. 20, no. 3, May-June 1983, pp. 249-256.

15. Adelman, Howard M.; Compiler: Computational Aspects of Heat Transfer in Structures. NASA CP 2216, 1982.

16. Beasley, Gary P.; Compiler: NASA Aircraft Controls Research 1983, NASA CP-2296, Oct. 1983.

17. Sobieski, Jaroslaw; Compiler: Recent Experiences in Multidisciplinary Analysis and Optimization. NASA CP 2327, April 1984.

18. Arrington, James P.; and Jones, Jim J.; Compilers: Shuttle Performance: Lessons Learned. NASA CP-2283, March 1983.

19. Chaffee, Norman; Compiler: Space Shuttle Technical Conference. NASA CP-2342, 1985.

20. Davis, John G. Jr.: Structures Technology Maturation for NASP (U). NASP TM 1017, May 1988.

21. Becker, J. V.: New Approaches to Hypersonic Aircraft. Presented at the Seventh Congress of the International Council of the Aeronautical Sciences (ICAS), Rome, Italy, Sept. 1970.

22. Shideler, J. L.; Swegle, A. R.; and Fields, R. A.: Honeycomb Sandwich Structure for Future Space Transportation Systems with Integral Cryogenic Tankage. Journal of Spacecraft and Rockets, vol. 21, no. 3, May-June 1984, p 246-252.

23. Shideler, J. L.; Webb, G. L.; and Pittman, C. M.: Verification Tests of Durable Thermal Protection System Concepts. Journal of Spacecraft and Rockets, vol. 22, no. 6, Nov. - Dec. 1985, pp. 598-604.

24. Camarda, Charles J.; and Basiulis, Al: Radiant Heating Tests of Several Liquid-Metal Heat-Pipe Sandwich Panels. Journal of Spacecraft and Rockets, vol. 21, no. 1, Jan. - Feb. 1984, pp. 4-5.

25. Wieting, Allan R.; Dechaumphai, Pramote; Bey, Kim S.; Thornton, Earl A.; and Morgan, Ken: Application of Integrated Fluid-Thermal-Structural Analysis Methods. Presented at the Congress of the International Council of the Aeronautic Sciences (ICAS), Jerusalem, Israel, Sept. 1988.

26. Dechaumphai, Pramote; Thornton, Earl A.; and Wieting, Allan R.: Flow-Thermal-Structural Study of Aerodynamically Heated Leading Edges. AIAA Paper No. 88-2245-CP, April 1988.

27. Camarda, Charles J; and McGowan, David M: Leading Edges for NASP - A Status Report. 4th NASP Technical Symposium, Feb. 17-19, 1988. NASA CP 4027, vol. 6, Paper No. 24.

28. Stein, Bland A.; Maahs, Howard G.; and Brewer, William D: Airframe Materials for Hypersonic Vehicles. NASA CP 2482, Metal-Matrix, Carbon, and Ceramic Matrix Composites, Edited by J. D. Buckley, 1987, pp. 1-28.

29. Williams, Robert M.: National Aero-Space Plane: Technology for America's Future. Aerospace America, Nov. 1986, p. 18.

30. Royster, Dick M; and Lisagor, W. Barry: Effect of High-Temperature and Oxidation on Residual Room-Temperature Properties for Several Thin-Sheet Superalloys. NASA TN D-6893, Nov. 1972.

31. Clark, Ronald K.; Cunnington, George R.; and Robinson, John C.,: Vapor Deposited Emittance/Catalysis Coatings for Superalloys in Heat Shield Applications. J. Thermophysics and Heat Transfer, vol. 1, no. 1, 1987, pp. 28-34.

32. Stoloff, N. S.; and Davies, R. G.: The Mechanical Properties of Ordered Alloys. Prog. Mater. Sci., vol. 13, no. 1, 1966, pp. 1-34.

33. Liu, C. T.: Physical Metallurgy and Mechanical Properties of Ductile Ordered Alloys ($(Fe,Co,Ni)_3V$. Inter. Met. Rev., vol. 29, no. 3, 1984, pp. 168-194.

34. Lipsitt, Harry A.: Titanium Aluminides--An Overview. High Temperature Ordered Intermetallic Alloys, Proc. of Materials Research Society Symposium, vol. 39, 1985, pp. 351-364.

35. Rummler, Donald R.; Cerro, Jeffrey A.; and Dixon, S. C.: Structures and Materials Requirements for Reusable Hypervelocity Vehicles. Presented at the Seventh Metal Matrix Composites Technology Conference, Naval Weapons Center, Silver Spring, MD, May 26-28, 1987.

36. Johnson, W. S.; Lubowinski, S. J.; Highsmith, A. L.; Brewer, W. D.; and Hoogstraten, C. A.: Mechanical Characterization of SCS_6/Ti-15-3 Metal Matrix Composites at Room Temperature. NASP TM 1014, April 1988.

37. Johnson, W. S.: Fatigue Testing and Damage Development in Continuous Fiber Reinforced Metal Matrix Composites , Metal Matrix Composites: Testing, Analysis and Failure Modes, ASTM STP 1032, In publication.

38. Bretz, Philip E.: Alithalite Alloys: 1987 Update. Aluminum-Lithium Alloys: Design, Development and Application Update, Conference Proceedings Edited by Ramesh J. Kar, Suphal P. Agrawal, and William E. Quist, ASM International, 1987.

39. Grimes, R.; Miller, W. S.; and Reynolds, M. A.: The Status of Alcan's Aluminum-Lithium Alloy Programme. Aluminum-Lithium Alloys: Design, Development and Application Update, Conference Proceedings Edited by Ramesh J. Kar, Suphal P. Agrawal, and William E. Quist, ASM International, 1987.

40. Blackburn, Linda A.; Casada, William; Colvin, Greg; Shiflet, Gary; and Starke, Edgar: The Effect of Processing on the Microstructure, Strength and Fracture Behavior of Aluminum-Lithium Alloys. Aluminum-Lithium Alloys: Design, Development and Application Update, Conference Proceedings Edited by Ramesh J. Kar, Suphal P. Agrawal, and William E. Quist, ASM International, 1987.

41. Pickens, Joseph R.; Henbaum, Frank A.; Kramer, Lawrence S.; Langan, Timothy J.; and Kumar, K. Sharvan: Weldalite® 049-Ultra-High-Strength Weldable Al-Li Alloy Development by Martin-Marietta. Military Handbook 5 Meeting, April 17, 1988, City of Industry, CA.

42. Skinner, D. J.; Rye, R. L.; Raybould, D.; and Brown, A. M.: Dispersion Strengthened Al-Fe-V-Si Alloys. Scripta Metallurgica, vol. 20, 1986, pp. 867-872.

43. Sanders, R. E., Jr.; and Hildemann, G. J.: Elevated Temperature Aluminum Alloy Development. Report No. AFWAL-TR-81-4076, Air Force Contract No. F33615-77-C-5086, 1981.

44. Adams, C. M.; Simon, J. W.; and Langenbeck, S.: Applications of Rapidly Solidified Aluminum Alloys at Elevated Temperatures. Third Conference on Rapid Solidification Processing--Principles and Technologies, December 1982.

45. Bales, T. T.; Hoffman, E. K.; Bird, R. K.; and Wiant, H. R.: Fabrication and Evaluation of Lightweight Ti_XAl Honeycomb Sandwich Panels by Enhanced Diffusion Bonding (U). Fourth National Aero-Space Plane Technology Symposium, Paper No. 74, Feb. 17-19, 1988.

46. Woodward, J. R.: Liquid Interface Diffusion Method of Bonding Titanium and/or Titanium Alloy Structure. U.S. Patent 3,957,194, May 18, 1976.

47. Massalski, T. B.: Binary Alloy Phase Diagrams. American Society for Metals, 1986.

48. Lindh, D. V.; Elrod, S. D.; and Lovell, D. T.: SST Technology Follow-on Program - Phase II, Development and Evaluation of the Aluminum-Brazed Titanium System; Volume IV - Material Properties. FAA-SS-73-5-4, 1974.

49. Hydrogen Embrittlement Testing. Symposium presented at the 75th Annual Meeting, American Society for Testing and Materials, June 25-30, 1972, ASTM STP 543.

50. Nelson, Howard G.; and Shanabarger, Mickey R.: Summary Proceedings of the Workshop on Hydrogen-Material Interactions (U). NASP Workshop Publication 1001, Aug. 1987.

51. Clark, R. K.; Wiedemann, Karl E.; Sankaran, Sankara N.; and Wallace, Terryl A.: Emittance, Catalysis, and Oxidation of TixAl and Coatings Under Hypersonic Conditions (U). 4th NASP Technical Symposium, NASA CP 4025, vol. 4, Paper No. 73A, Feb. 17-19, 1988.

52. Schaefer, John W.; Tong, Henry; Clark, Kimble J.; Suchsland, Kurt E.; and Neuner, Gary J.: Analytic and Experimental Evaluation of Flowing Air Test Conditions for Selected Metallics in a Shuttle TPS Application. NASA CR-2531, 1975.

53. Touloukian, Y. S.; and Dewitt, D. P., eds.: Thermal Radiative Properties--Nonmetallic Solids. IFI/Plenum, 1972

54. Curry, D. M.: Carbon-Carbon Materials Development and Flight Certification Experience From Space Shuttle. NASA Conference Publication 2501, 1988, In publication.

55. H. G. Maahs, ed., Oxidation-Resistance Carbon-Carbon Composites for Hypersonic Vehicle Applications. NASA Conference Publication 2501, 1988, In Publication.

56. Air Force Technical Objective Document FY88, AFWAL-0TR-86-4000, 1986.

57. Maahs, Howard G.; Ohlhorst, Craig W.; Barrett, David M.; Ransone, Philip O.; and Sawyer, J. Wayne: Response of Carbon-Carbon Composites to Challenging Environments. Proceedings of MRS Symposium, Spring 1988.

58. Rogers, D. C.; Seegr, J. W.; and Shuford, D. M.: 18th National SAMPE Symposium and Exhibition, vol. 16 (Society for the Advancement of Materials and Process Engineer, 1973), pp. 202-216)

59. Stroud, C. W.; and Rummler, D. R.: Mass Loss of a TEOS-Coated, Reinforced Carbon-Carbon Composite Subjected to a Simulated Shuttle Entry Environment. NASA TM-81799, 1980.

60. Stroud, C. W.; and Rummler, D. R.: Mass Loss of TEOS-Coated RCC Subjected to lthe Environment at the Shuttle Wing Lerading Edge. NASA TM-83203, 1981.

61. Clarke, W. A.; Eitman, D. A.; Ketterer, M. E.; and Wesley, J. L.: Inhibited Filament, Oxidation-Resistant Carbon-Carbon Composites. NASA Contractor Report 178177, 1986.

62. Scott, R. O.; Shuford, C. M.; Webster, C. N.; and Payne, C. W.: Development of Advanced Carbon-Carbon (ACC) Composites - Materials Development. NASA CR165842-1, vol. 1, July 1982.

63. Rummler, D. R.: ACC Materials Research. Advancements in TPS and Structures for Space Transportation Systems, H. N. Kelly and J. E. Gardner, Compilers, Proceedings of a Symposium held at NASA Langley Research Center, December 13-15, 1983, NASA CP-2315,.pp. 399-410.

64. Ohlhorst, C. W.; and Ransone, P. O.: Effects of Thermal Cycling on Thermal Expansion and Mechanical Properties of Advanced Carbon-Carbon Composites. Metal-Matrix, Carbon-, and Ceramic-Matrix Composites, J. D. Buckley, Ed., Proceedings of a Joint NASA/DOD Conference, Cocoa Beach, FL, Jan. 23-25, 1985, NASA CP-2406,.pp. 277-288.